

Lead-up and manifestation of the Oceanic Anoxic Event 2 at the DSDP Site 398 (Vigo Seamount, NW Iberian offshore): Palynological and geochemical insights

Iván Rodríguez-Barreiro^{a,b,*}, Artai A. Santos^c, Uxue Villanueva-Amadoz^d, Stephen Louwye^e, Stuart A. Robinson^f, José B. Diez^{a,b}

^a Centro de Investigaciones Mariñas, Universidade de Vigo, BASAN, Vigo 36310, Spain

^b Departamento de Xeociencias Mariñas e Ordenación do Territorio, Universidade de Vigo, Vigo 36310, Spain

^c Department of Palaeobiology, Swedish Museum of Natural History, SE-104-05 Stockholm, Sweden

^d Estación Regional del Noroeste (ERNO), Instituto de Geología, UNAM, Hermosillo 83000, Mexico

^e Department of Geology, Ghent University, Ghent, Belgium

^f Department of Earth Sciences, University of Oxford, Oxford, UK

ARTICLE INFO

Editor name: Dr. Bing Shen

Keywords:

Paleopalynology
Cenomanian-Turonian Boundary Event
Bonarelli Event
Black shales
Hatteras Formation
Mid-Cretaceous

ABSTRACT

Extreme climatic conditions, volcanism, and paleogeographical distribution presumably led to the Oceanic Anoxic Event 2 (OAE 2), one of the most disruptive events for Cretaceous ecosystems. Although the terrestrial response to this issue is barely studied, a turnover within the plant communities seems to be linked to the OAE 2, besides the well-known extinction of several marine groups. In this study, palynological and $\delta^{13}\text{C}_{\text{org}}$ analyses were combined to research the sediments from DSDP Site 398 (Vigo Seamount) cores 398D-58 to 398D-56 (upper Albian to lower Turonian). The $\delta^{13}\text{C}_{\text{org}}$ curve exhibits a Carbon Isotopic Excursion (CIE) observed between the interval 948,60 and 947,77 m below seafloor (mbsf), corresponding to the OAE 2. Four palynological assemblages were differentiated, ranging from the uppermost Albian to the lower Turonian. These assemblages comprised diverse marine and terrestrial communities with generally excellent preservation. In addition to previous biostratigraphic works, we present a more detailed chronostratigraphy of DSDP Hole 398D based on palynomorphs. The paleoecological reconstruction reveals the significant changes during the OAE 2 period: a decrease in the diversity and abundance of dinoflagellate cysts and a shift to angiosperm-dominated terrestrial communities (i.e., Normapolles) which, unlike other sites, occurs prior to the maximum values of $\delta^{13}\text{C}$.

1. Introduction

Oceanic Anoxic Events (OAEs; Schlanger and Jenkyns, 1976) were major oceanographic crises related to perturbations of the long-term global carbon cycle in the Cretaceous. These OAEs are usually recognized in the geological record as a widespread occurrence of black shales, formed by the deposition of organic carbon-rich sediments in marine environments during a relatively short period, and usually correspond to a positive carbon-isotope ($\delta^{13}\text{C}$) excursion (Scholle and Arthur, 1980; Arthur et al., 1987). During the Cenomanian–Turonian boundary, a pronounced OAE was recorded worldwide with an estimated duration between 0.5 and 1 Ma (Meyers et al., 2012; Li et al., 2017; Gangl et al., 2019; Boulila et al., 2020), known as the Bonarelli

Event, the Oceanic Anoxic Event 2 (OAE 2), or the Cenomanian–Turonian Boundary Event (CTBE). The climatic and oceanographic changes associated with the OAE 2 disturbed both terrestrial and marine ecosystems worldwide (Kuypers et al., 1999; Monnet, 2009; Fischer et al., 2016; Heimhofer et al., 2018).

The Cenomanian–Turonian time interval was characterized by extreme climatic conditions. Atmospheric CO_2 levels and temperatures were abnormally high during this time (Freeman and Hayes, 1992; Jenkyns et al., 1994; Follmi, 1995; Retallack, 2001; Huber et al., 2002; Hong and Lee, 2012; Witkowski et al., 2018) while sea level was at its highest of all the Cretaceous (Haq, 2014) due to a lack of substantial continental ice volume (Sames et al., 2016). The hydrological cycle was likely invigorated into this greenhouse climate, leading to enhanced

* Corresponding author at: Centro de Investigaciones Mariñas, Universidade de Vigo, BASAN, Vigo 36310, Spain.

E-mail address: ivan.rodriguez.barreiro@uvigo.gal (I. Rodríguez-Barreiro).

<https://doi.org/10.1016/j.palaeo.2024.112223>

Received 7 November 2023; Received in revised form 8 March 2024; Accepted 21 April 2024

Available online 24 April 2024

0031-0182/© 2024 The Authors. Published by Elsevier B.V. This is an open access article under the CC BY-NC license (<http://creativecommons.org/licenses/by-nc/4.0/>).

runoff and increased global weathering rates that, in turn, caused increased nutrient supply and stratification in the oceans (Jenkyns, 1980; van Helmond et al., 2014a, 2014b). Large Igneous Province (LIP) volcanism (i.e., Caribbean and High Arctic LIPs) occurred coeval with the onset of OAE 2 (Sinton and Duncan, 1997; Kerr, 1998; Snow et al., 2005; Turgeon and Creaser, 2008) and drove a series of environmental perturbations that led to widespread organic carbon burial (Jenkyns, 2010; Robinson et al., 2017, 2019; Li et al., 2022).

The environmental perturbations leading to the OAE 2 certainly had an effect over the terrestrial ecosystems as well. Increased plant productivity and terrestrial runoff may have contributed to nutrient availability in marine settings (Barclay et al., 2010; Lowery et al., 2021) which, at the same time, enhanced primary production in marine environments leading to a more efficient removal of oxygen from the proto-Atlantic (Monteiro et al., 2012; Boudinot et al., 2021). Although the response of the continental ecosystems to the extreme mid-Cretaceous climate should be addressed, studies of these floral changes are scarce yet (Kuypers et al., 1999; Heimhofer et al., 2018; Laurin et al., 2019; Galasso et al., 2023).

In the proto-North and South Atlantic, there are several drilling sites where the OAE 2 has been identified. Two of these are offshore on the Iberian Margin, specifically on the Vigo Seamount and Galicia Bank (DSDP sites 398 and 641, respectively; Fig. 1). These sites represent the OAE 2 in a location with unique conditions. The sedimentary source was the NW Iberian Peninsula (an island by then) bordered by the Tethyan Seaway to the south (Laugié et al., 2021). The sites were located in the subtropical zone and, therefore, were sensitive to climatic changes (e.g., Barron et al., 1995). Thus, the sites potentially provide the opportunity to examine the response of terrestrial and marine ecosystems to the OAE 2.

Although several micropaleontological studies have been carried out at these two sites, principally for biostratigraphic purposes (Bleischmidt, 1979; Sigal, 1979; Moullade et al., 1988; Thurow, 1988; Thurow et al., 1988), Site 398 lacks any micropaleontological research on sporomorph assemblages focused on the OAE 2 that could reveal the response of plant communities on land. Moreover, the Cenomanian–Turonian chronostratigraphy of Hole 398D is inaccurate, and chemostratigraphical analyses are missing. Therefore, the aims of this work are: 1) to confirm the presence of the OAE 2 at Site 398 using

$\delta^{13}\text{C}_{\text{org}}$; 2) to establish a detailed palynological zonation and compare it with previous chronostratigraphical records; 3) to reconstruct the paleoecology of the continental and marine plant/phytoplankton communities based on the palynological content (organic-walled microfossils); 4) to elucidate if there is any significant paleoecological or paleoenvironmental response to the OAE 2.

1.1. Geological context

The sediments from Site 398 were recovered in 1976 by the Deep Sea Drilling Project (DSDP) during Leg 47B (Ryan et al., 1979a) on the southern flank of the Vigo Seamount (Fig. 1). The middle to uppermost Cretaceous sediments recovered from Hole 398D were divided into three different lithological subunits (3A, 3B, and 4A) corresponding to the Plantagenet (3A and 3B) and Lithological subunit (4A) formations (Fig. 2).

The lithologies of Subunit 4A, spanning 947 to 1192,5 mbsf, consist of greyish-green marly nannofossil cherts to calcareous mudstones, interbedded with dark grey to greyish-black mudstones (black shales) and a few thin radiolarian sands in the upper part (Ryan et al., 1979b). The subunit 4A is interpreted as hemipelagic-pelagic deposition, characterized by rhythmic bedding and fluctuating carbonate and organic carbon contents, periodic anoxia, or deficient bottom water oxygenation. The seafloor had probably been above the Carbonate Compensation Depth (CCD), but redeposition of carbonates from slopes does occur. There are three sediment sources (Arthur, 1979): 1) terrigenous input, mud turbidites, and hemipelagites; 2) pelagic carbonate input; 3) downslope redeposition of older and penecontemporaneous carbonate. The sedimentary supply is mainly continental in the lower part. At the same time, marine organic matter is dominant between 1088 and 974 mbsf, except in the uppermost part (964,5 to 945,5 mbsf), where terrigenous sediment is present again (Graciansky and Chenet, 1979).

The sharp contact between subunit 4A and the overlying subunit 3B (c. 947,20 mbsf) can be noticed in seismic profiles as a slight angular discordance, possibly due to erosion by a deep current (Arthur, 1979). The lithologies of subunit 3B are brown to yellowish-brown, dark reddish-brown, red, and reddish-grey non-fossiliferous mudstones and claystones, predominantly massive, homogeneous, and unburrowed, with rhythmic intercalations of thin silt and sand laminae (Ryan et al.,

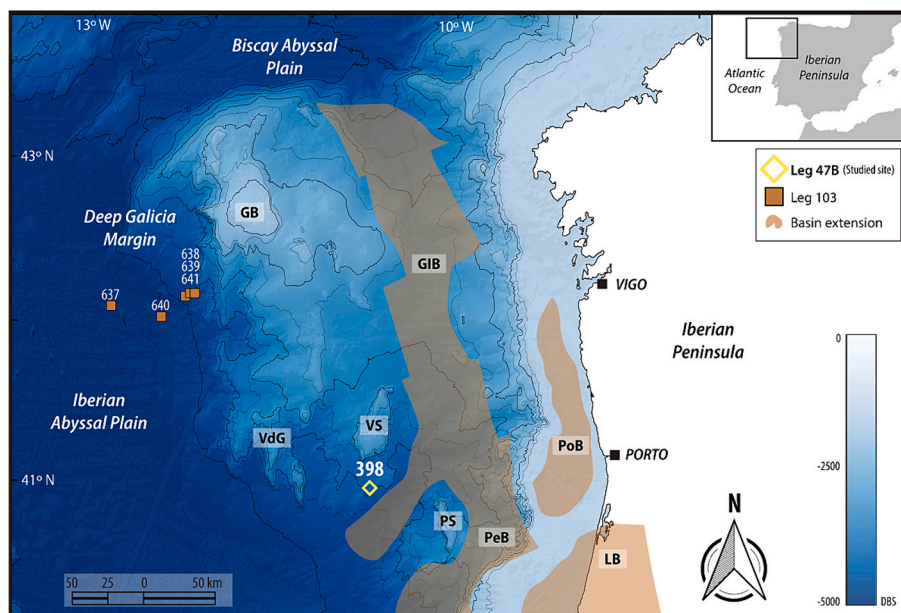
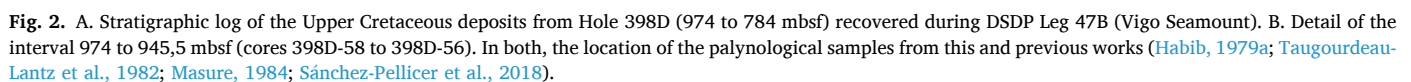


Fig. 1. Location of the Vigo Seamount and the nearby sedimentary basins. GB: Galicia Bank; GIB: Galicia Interior Basin; VdG: Vasco de Gama Seamount; VS: Vigo Seamount; PS: Porto Seamount; PeB: Peniche Basin; PoB: Porto Basin; LB: Lusitanian Basin. Location of the sedimentary basins based on Murillas et al. (1990) and Alves et al. (2009).



1.2. Biostratigraphic and geochemical background

Cenomanian and upper Albian age, respectively. However, the first assemblage is poorly preserved; from 950,0 mbsf to the top of the studied interval no nannofossils are recorded (Blechschmidt, 1979). Thurow (1988) re-examined the radiolarians from the OAE 2 interval, dating the upper part of the studied section to a younger age than previously thought (upper Cenomanian–lower Turonian).

The few Cretaceous palynological studies were not focused on the OAE 2. [Habib \(1979a, 1979b\)](#) studied the general patterns of terrestrial palynology, the palynofacies, and the origin of the sediments from the Hauterivian to Cenomanian age. Marine palynological works had a more general perspective ([Masure, 1984](#)) and were compared to other sections from the Portuguese coast ([Taugourdeau-Lantz et al., 1982](#); [Sánchez-Pellicer et al., 2018](#)).

Mineralogical and geochemical studies from Site 398 include spectrophotometric analysis (Chamley et al., 1979), organic carbon

characterization (Deroo et al., 1979; Herbin et al., 1986), as well as carbon and oxygen isotopic analysis (Arthur et al., 1979; Letolle, 1979). Nevertheless, for the latter, no samples were analyzed along the OAE 2 sediments.

2. Materials and methods

2.1. Palynological analysis

A total of 49 samples from cores 398D-58 to 398D-40, provided by the Bremen Core Repository, were analyzed. After the palynological treatment, 24 samples yielded palynomorphs, all of them from the Hatteras Formation (between 966,82 and 948,10 mbsf).

The samples were processed in the laboratory of Paleobotany at the University of Vigo using the standard palynological technique of HCl–HF–HCl described by Wood et al. (1996), which consists of acid digestion to remove carbonate and silicate minerals. A dispersing agent was subsequently added to facilitate filtering with a five μm sieve. The residues were mounted on glass slides and were studied under a LEICA DM 2000 LED optical microscope equipped with a LEICA ICC50 W digital camera. For SEM observation, after the standard palynological treatment, the organic residue of three palynological samples (Sample codes 47B-01, 47B-15, and 47B-26 in Fig. 2) was dried and coated with gold nanoparticles before examination under the Scanning Electron Microscope (SEM) JEOL JSM6010LA (JEOL Ltd., Tokyo, Japan) at CACTI facilities (Centro de Apoio Científico-Tecnológico á Investigación, University of Vigo). The illustrated specimens are indicated by the fossil taxa name followed by sample number, slide number, and England Finder reference. The samples are stored in the laboratory of Palynology, Department of Marine Geosciences and Territorial Planning, University of Vigo (Spain).

Quantitative analysis was conducted on all the samples, including a minimum of 250 palynomorphs counted per slide (see Supporting Information). The palynological counting and derived calculations were done separately for terrestrial and marine palynomorphs. Unless otherwise indicated, the biological affinities of the palynomorphs identified are based on the recompilation of botanical affinities by Zhang et al. (2021) for plant spores and pollen, and the main classification of Fensome et al. (1993) for dinoflagellate cysts. Although the data are shown in percentages, they should be considered qualitative as the taphonomy does not truly represent the biocenoses. The Palynological Marine Index (PMI) was calculated according to the richness (number of genera) of marine and terrestrial palynomorphs (Helenes et al., 1998). The Peridinioid/Gonyaulacoid ratio (P:G) is based on the formula proposed by Versteegh (1994), which is related to the ratio between heterotrophic and autotrophic dinoflagellates (Harland, 1973). The diversity was calculated using the Shannon-Wiener Index on a genus-rank level.

The palynological dating relies on selected taxa with restricted ranges around the Albian–Turonian interval based on different palynological studies located in the Normapolles Province (for the continental palynomorphs) and worldwide (for the dinoflagellate cysts). Unless otherwise indicated, only references with taxa illustrations and a clear stratigraphic assignment were included.

2.2. Carbon isotope

The carbon-isotope values of the bulk organic matter in sediment samples were analyzed using the dried residue after the acid digestion with HCl and HF from the previous palynological standard treatment. Samples were analyzed using the Isotopic Ratio Mass Spectrometry (IRMS) at the CACTI facilities (University of Vigo) with an elemental analyzer FlashEA 1112 Series (ThermoFinnigan) coupled with an Interface ConFlo III (ThermoFinnigan) to an isotopic ratio mass spectrometer MAT253 (ThermoFinnigan). In each analytical sequence, secondary standards used were IAEA-C-6 ($-10.8\text{‰} \pm 0.47$), IAEA CH7

($-32.15\text{‰} \pm 0.05$), and IAEA C3 ($-24.9\text{‰} \pm 0.04$). An average reproducibility for the bulk sample better than 0.3‰ ($\pm 1\sigma$, $n = 3$) was obtained. Carbon-isotope values were expressed in per mille (‰) deviation from VPDB (Vienna Pee Dee Belemnite) using the standard delta notation ($\delta^{13}\text{C}$).

3. Results

3.1. Palynology

A total of four palynological assemblages were differentiated (Figs. 3–5; see Supporting Information for the list of taxa, their stratigraphic distribution and further palynological illustrations): Assemblage A (966,82 to 961,87 mbsf), Assemblage B (961,23 to 956,13 mbsf), Assemblage C (952,04 to 950 mbsf), and Assemblage D (949,37 to 948,10 mbsf).

The Assemblage A has, in general, moderate preservation and diversity, which decreases at certain stratigraphic levels (i.e., interval 964,5 to 966 mbsf). The assemblage is dominated by Cheirolepidiaceae pollen, especially throughout the previous low-diversity interval (Fig. 3), and, in a lower proportion, Pinaceae-Podocarpaceae and Araucariaceae pollen. Occasionally, Schizaeales (putative Anemiaceae), Selaginellaceae, Cyatheaceae, and Marsileaceae have a significant presence. Marine elements are present in all samples (with c. 20% of relative abundance). *Pterodinium* and foraminiferal test linings are dominant, with a significant presence of *Circulodinium* and *Oligosphaeridium* dinoflagellate cysts. Towards the top (961,87 mbsf), the marine elements become more frequent (above 50%), showing the dominance of *Sepispinula*, *Litosphaeridium*, *Pterodinium*, and *Circulodinium* dinoflagellate cysts. Other palynomorphs like freshwater algae (*Schizosporis* sp.), prasinophycean algae (*Pleurozonaria* sp.), and putative Lepidopteran wing scales are also present in this assemblage.

The Assemblage B is marked by the first record of *Wilsonisporites woodbridgei* spore at 961,23 mbsf. It exhibits moderate to high diversity and moderate preservation. In the lower part, the continental fraction is dominated by Pinaceae-Podocarpaceae and Cheirolepidiaceae pollen as well as pteridophyte spores, mainly Selaginellaceae, Schizaeales (putative Anemiaceae), and Cyatheaceae, as well as occasionally Marsileaceae, Gleicheniaceae, and Lycopodiaceae. In contrast, a significant dominance of pteridophyte spores characterizes the upper part. The marine fraction is prominent in all productive samples (c. 20%) and mainly dominated by *Pterodinium*, with occasional relatively high dominances of other dinoflagellate cysts such as *Litosphaeridium*, *Spiniferites*, and *Sepispinula*. The relative abundance of the latter decreases towards the top until its Last Occurrence (LO) at 956,68 mbsf. Other palynomorphs, such as foraminiferal test linings and putative Lepidopteran wing scales, are also present.

The Assemblage C is marked by the first occurrence of Normapolles-group pollen at 952,04 mbsf. Preservation and diversity are moderate. The continental fraction is dominated by Pinaceae-Podocarpaceae and Cheirolepidiaceae pollen, as well as pteridophytes, mainly Schizaeales (putative Anemiaceae), Selaginellaceae, Cyatheaceae, and Lycopodiaceae. The marine elements, increasing towards the top of the assemblage, are dominated by *Pteridodinium*, *Spiniferites* and *Litosphaeridium* dinocysts, as well as the acritarch *Verhyachium* are occasional co-dominants. Other palynomorphs such as foraminiferal test linings, prasinophycean algae (*Tasmanites* sp.), and putative Lepidopteran wing scales are also present.

The Assemblage D is marked by the diversification of the Normapolles group pollen (the first record of several fossil species from *Atlantopolis*, *Complexiopolis*, *Minorpollis*, *Tenerina*, and *Triangulipollis*). Palynomorphs are well preserved but preservation decreases noticeably upwards (948,10 mbsf). The diversity is low to moderate. Angiosperm pollen from the Normapolles group are dominant (mainly *Atlantopolis* and *Complexiopolis*; i.e., Myricaceae), reaching up to 80% in some levels (Fig. 3). Also well represented are Chloranthaceae and Pinaceae-

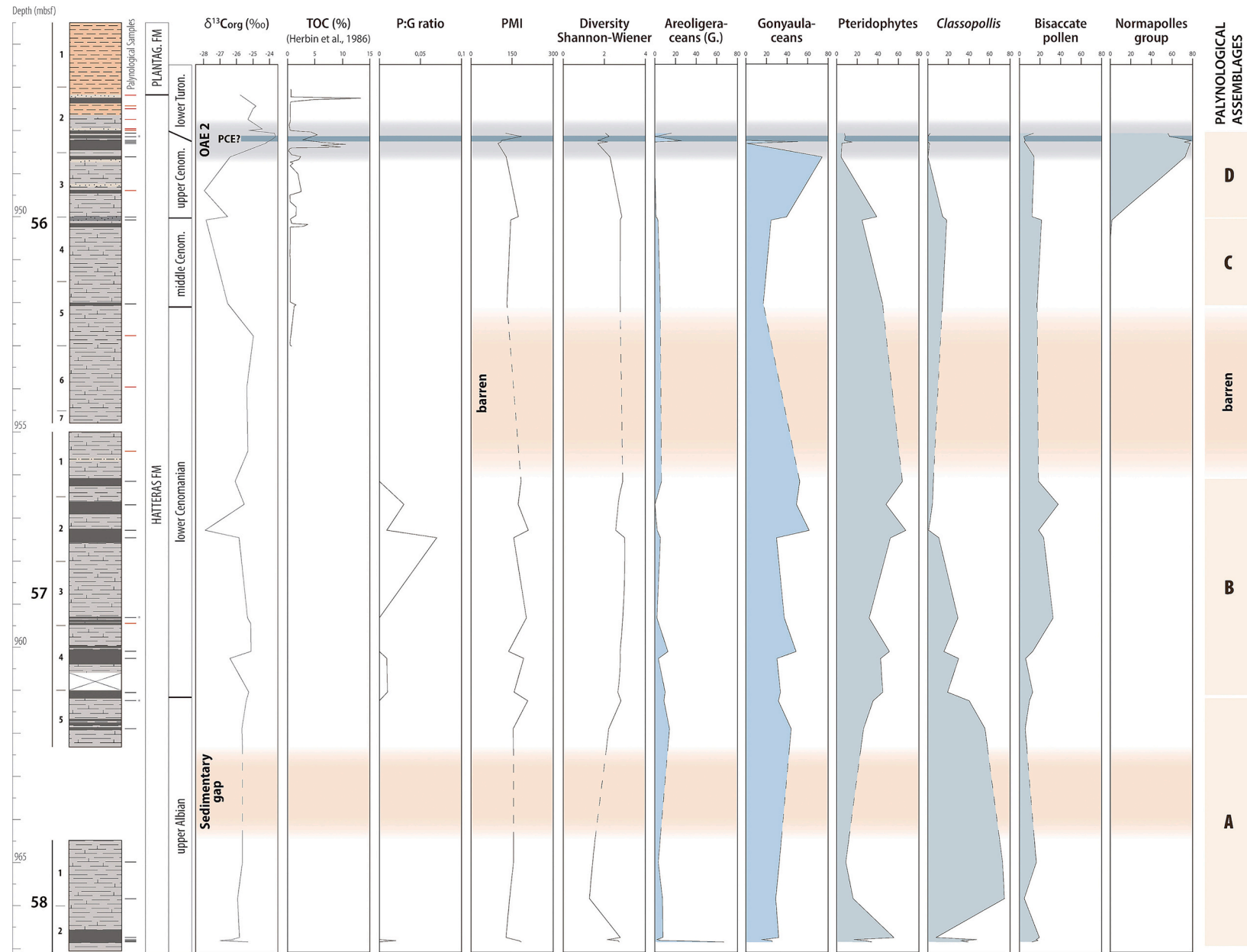


Fig. 3. Geochemical and palynological results. The grey band corresponds to the OAE 2 and the inner blue band to the possible location of the Plenus Cold Event (PCE). The orange band corresponds to a palynological barren zone and a sedimentary gap, respectively. The Total Organic Carbon (TOC) data were taken from [Herbin et al. \(1986\)](#). The samples with “*” are low in abundance (counting <250 palynomorphs). Legend for the stratigraphic log in [Fig. 2](#). (For interpretation of the references to colour in this figure legend, the reader is referred to the web version of this article.)



Fig. 4. Representative selection of the palynological assemblages from the DSDP Hole 398D (966,82 and 948,10 mbsf interval): a, *Cyathidites minor* (47B-04-1-E250); b-c, *Patellasperites distaverrucosus* (47B-26-2-S313); d, *Crybelosporites pannuceus* (47B-02-1-O230); e, i, *Wilsonisporites woodbridgei* (47B-08-1-Q152); f, *Plicatella* cf. *crickmayii* (47B-15-4-L223); g, *Cicatricosisporites purbeckensis* (47B-04-1-H321); h, *Camarozonosporites dakotaensis* (47B-15-1-L383); j, *Classopollis classoides* (47B-15-1-R211); k, *Podocarpidites granulosus* (47B-11-1-J384); l, *Quadricolpites* sp. (47B-01-3-H501); m, *Minorpollis minimus* (47B-23-3-H103); n, *Complexiopollis complicatus* (47B-23-3-J452); o, *Atlantopollis heystii* (47B-26-1-C203); p, *Atlantopollis reticulatus* (47B-24-1-M451); q, *Complexiopollis praeatutenscens* (47B-26-1-J322); r, *Complexiopollis vancampoe* (47B-26-2-H194); s, *Complexiopollis* sp. (47B-19-1-M274); t, *Trudopollis pertrudens* (47B-26-1-P352); u, *Asteropollis vulgaris* (47B-24-1-H113); v, *Tricolpites barrandei* (47B-20-1-D321); w, *Dichastopollenites dunveganensis* (47B-11-1-L282). See Supporting Information for complementary illustrations.

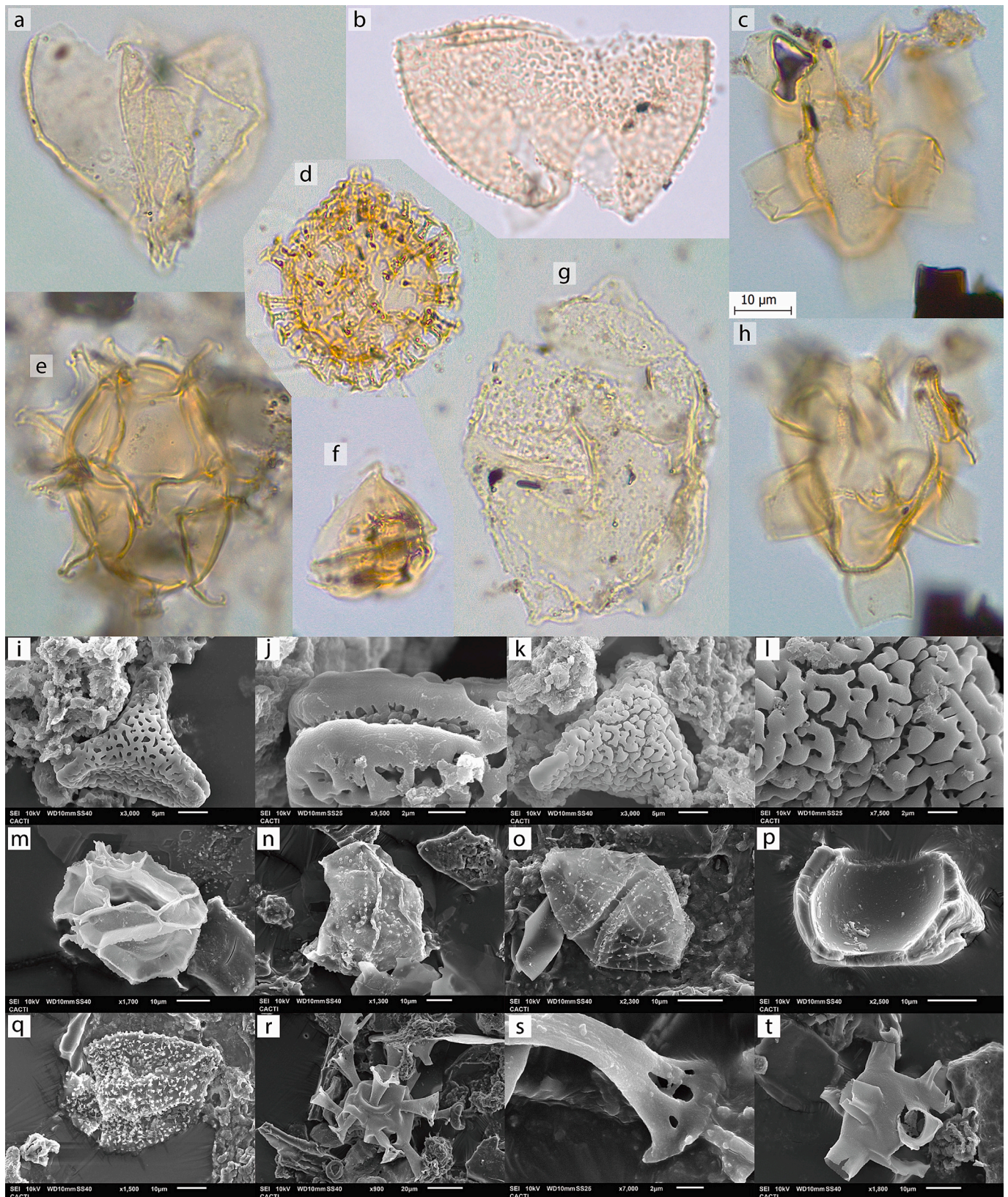


Fig. 5. Representative selection of the palynological assemblages from the DSDP Hole 398D (966,82 and 948,10 mbsf interval): a, *Circulodinium colliveri* (47B-11-1-C473); b, *Circulodinium brevispinosum* (47B-28-4-D244); c, h, *Litosphaeridium siphoniphorum* (47B-15-1-N144); d, *Sepispinula ancorifera* (47B-10-1-T121); e, *Spiniferites* sp. (47B-06-1-N141); f, cf. *Dinogymnium* sp. (47B-02-1-L450); g, *Ovoidinium verrucosum* (47B-09-1-E111); i-j, *Atlantopollis reticulatus* and detail to its germinal protrusion (47B-26); k-l, *Atlantopollis heystii* and detail to its ornamentation (47B-26); m, *Pterodinium cingulata* (47B-15); n, *Cerbia tabulata* (47B-15); o, *Canninginopsis denticulata* (47B-01); p, *Cauveridinium membraniphorum* (47B-15); q, *Circulodinium brevispinosum* (47B-01); r-s, *Oligosphaeridium pulcherrimum* and detail to its processes (47B-15); t, *Litosphaeridium siphoniphorum* (47B-15). See Supporting Information for complementary illustrations.

3.2. Carbon isotope

The $\delta^{13}\text{C}_{\text{org}}$ curve through the studied section is shown in Fig. 3. From the base of the studied section to 948,60 mbsf, values are between -28.0 and -23.7% with a general trend to lower values towards the

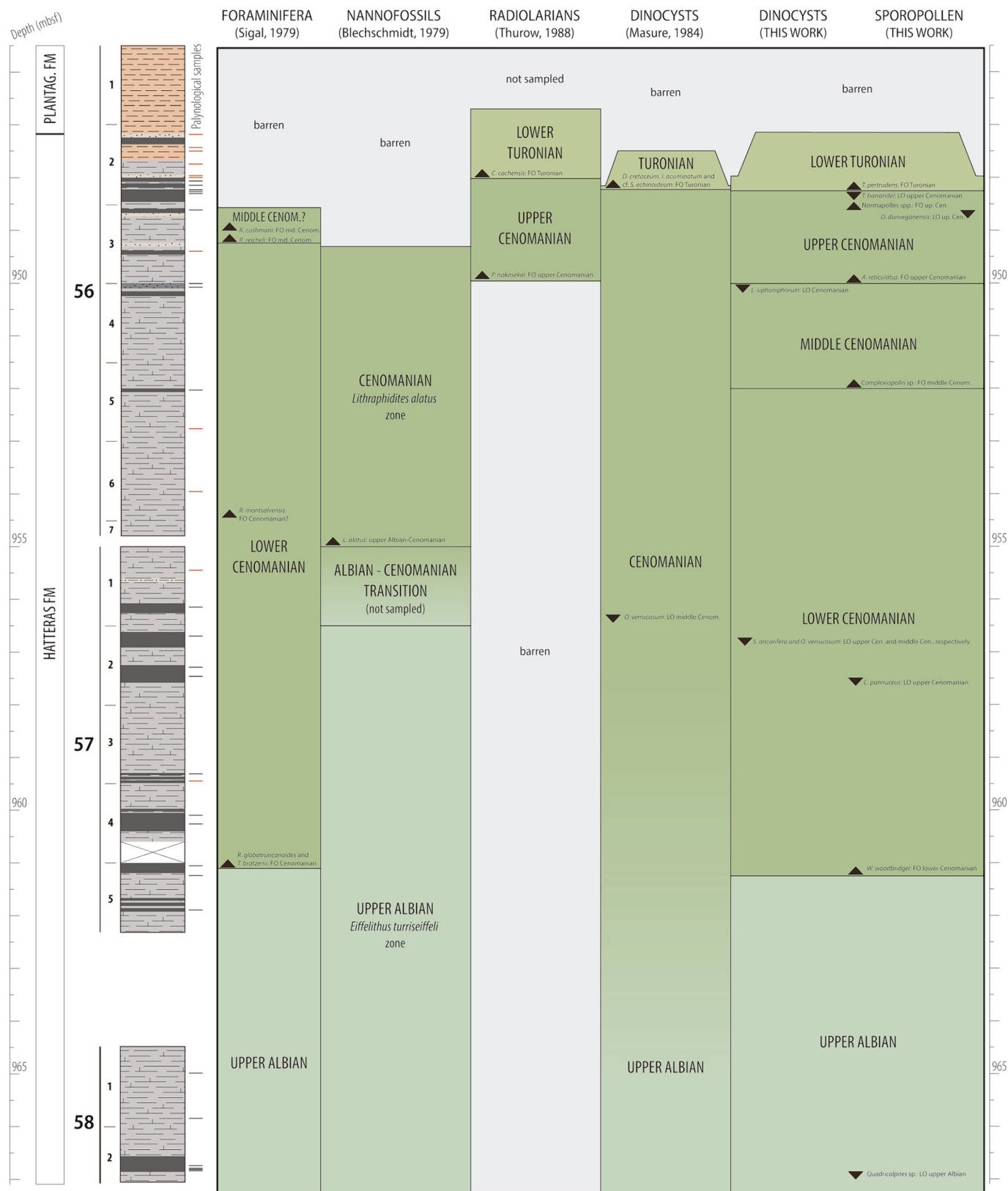


Fig. 6. Synthesis of the biostratigraphy for the Vigo Seamount, including the new data provided by this work. Legend for the stratigraphic log in Fig. 2.

upper part. However, a clear positive excursion is found from this point (948,60 mbsf upwards), with maximum $\delta^{13}\text{C}_{\text{org}}$ values of -24.3 and -23.6‰ in the interval between 948,31 and 948,10 mbsf. It should be noted that the interval 947,20 to 947,43 mbsf was depleted, but another black shale level is found of about 5 cm thick which contains the highest TOC levels of the studied cores (Herbin et al., 1986). Therefore, the stratigraphic top of the $\delta^{13}\text{C}$ positive excursion cannot yet be determined, but may be somewhere within that interval.

3.3. Biodiversity and palynological indicators

Several ratios and indexes were calculated to aid the interpretation of the paleoecosystem and its changes through the Albian–Turonian interval.

The Palynological Marine Index (PMI) showed a steady trend with an average value of c. 150, ranging between 100 (OAE 2) and 214,29 (palynological assemblage B). Slight variations were mainly found throughout the palynological assemblage B (Fig. 3).

The Peridinioid/Gonyaulacoid ratio (P:G) is low throughout the studied section, with values close to zero. However, this ratio peaks at the upper part of palynological assemblage B, reaching a value of c. 0.07.

According to the Shannon–Wiener Index, biodiversity can be divided into three stages. First, corresponding to the palynological assemblage A, low diversity values (<2) are found as a result of *Classopollis*-dominated microfloras (Fig. 3). Then, an increase in biodiversity (values around 3) is found in palynological assemblage B and C. Eventually, another biodiversity drop corresponds to the palynological assemblage D, mainly produced by the Normapolles-dominated microfloras.

4. Discussion

4.1. Stratigraphical assessment

4.1.1. Palynostratigraphy of Site 398

According to the stratigraphic ranges of selected taxa (both marine and continental), we suggest the age of each palynological assemblage (Fig. 6).

The Assemblage A of this study follows the uppermost Albian interval from Hole 398D upsection studied previously (*Palinostratigraphic Unit VI* of Habib, 1979a; Taugourdeau-Lantz et al., 1982; Masure, 1984; Sánchez-Pellicer et al., 2018). The suggested age for this assemblage is also upper Albian according to the First Occurrence (FO) of *Litospheeridium siphoniphorum* considered as a marker of the beginning of the upper Albian (Fauconnier, 1975; Powell, 1992; Williams, 1993; Duxbury, 2001; Williams et al., 2004) and the Last Occurrence (LO) of *Quadricolpites* sp. at 966,82 mbsf, which is regarded to represent the uppermost Albian (Wingate, 1980; Ward, 1986; Ravn, 1995; Villanueva-Amadoz, 2009). There are some taxa whose presence in Assemblage A is problematic, such as *Cicatricosisporites purbeckensis* and cf. *Dinogymnium* sp. (see Supporting Information for a detailed discussion about key taxa and others).

The top of Assemblage A is at the lower part of core 57, where the Albian–Cenomanian boundary would be located at 961,23 mbsf. This proposal is consistent with the age suggested by foraminifera (Sigal, 1979), placing the beginning of the Cenomanian at 961,08 mbsf according to the FO of *Thalmaninella globotruncanoides*, which is used as a primary marker for the base of the Cenomanian GSSP (Kennedy et al., 2004). Regarding the nannofossil studies, Blechschmidt (1979) suggests that the Albian–Cenomanian boundary should be located in the 955–956,5 mbsf interval between the *Lithraphidites alatus* (Cenomanian) and *Eiffelithus turriseiffeli* (upper Albian) biozones. However, the preservation grade of the former biozone is poor (Blechschmidt, 1979), resulting in a lack of precision.

A lower Cenomanian is suggested for the Assemblage B according to the FO of *Wilsonisporites woodbridgei* in the lower Cenomanian (Kimyai, 1966, 1970; Azéma et al., 1990; Peyrot et al., 2019) and the LO of

Ovoidinium verrucosum at the lower–middle Cenomanian boundary (Leereveldt, 1995; Williams et al., 2004). However, two Cenomanian key taxa (*Sepispinula ancorifera* and *Crybelosporites pannuceus*) seem to have their LOs earlier in Site 398 than in other regions, and there is an unexpected presence of *Plicatella crickmayi*, which will have new stratigraphic implications (see Supporting Information for a detailed discussion about key taxa and others).

The lower–middle Cenomanian boundary is positioned at 952,04 mbsf. This position is stratigraphically lower than the one proposed by foraminifera, according to the FO of *Rotalipora cushmani* and *Thalmaninella reicheli* at 948,95 and 949,26 mbsf, respectively (Sigal, 1979). However, from 950,50 upwards, the preservation of the assemblage decreases (Sigal, 1979), which can affect the recognition of foraminifera and, therefore, not exclude the earlier presence of middle Cenomanian markers, as suggested by our palynological study (Fig. 6).

A middle Cenomanian age of Assemblage C is suggested by the presence of the *Complexiopollis* genus. In Hole 398D, the first record of Normapolles-group pollen (i.e., *Complexiopollis* sp.) occurs at 952,04 mbsf, marking the beginning of the middle Cenomanian according to its FO (Pactová, 1971; Louail et al., 1978).

The middle–upper Cenomanian boundary is at the top of core 56–4. This age assignment is consistent with the radiolarian dating, which suggests an upper Cenomanian age assemblage for the interval 949,99 to 948,02 mbsf (Thurrow, 1988) (Fig. 6).

The Assemblage D corresponds to an upper Cenomanian–lower Turonian age since several Normapolles-group pollen have their FOs in the upper Cenomanian, such as *Atlantopollis heystii*, *A. reticulatus*, *Complexiopollis complicatus*, *C. vancampoe*, *C. praeatuescens*, and *Minorpollis* sp. (van Amerom, 1965; Antonescu, 1973; Robbins et al., 1975; Christopher, 1977; Kedves and Diniz, 1979; Kedves, 1980; Azéma et al., 1981; Herngreen and Chlonova, 1981; Hochuli, 1981; Thurrow et al., 1988; Fechner and Dargel, 1989; Batten and Marshall, 1991; Peyrot et al., 2008; Peyrot et al., 2011; Pavlishina and Wagreich, 2012). The Cenomanian–Turonian boundary should be located, according to palynostratigraphy, at 948,23 mbsf, as some key taxa present below and above this stratigraphic level differentiate the Cenomanian from the Turonian: the LOs of *Dichastopollenites dunveganensis* and *Tricolpites barrandei* (both recorded at 948,27 mbsf) in the uppermost Cenomanian (Azéma et al., 1990; Uličný et al., 1997; Ibrahim et al., 2020), and the FO of *Trudopollis pertrudens* (recorded at 948,23 mbsf) in the lower Turonian (Azéma et al., 1981).

Based on palynology, the Cenomanian–Turonian boundary is located between 948,23 and 948,27 mbsf, which is consistent with previous palynological studies (Masure, 1984) according to the FO of *Dinogymnium cretaceum*, *Isabelidinium acuminatum*, and cf. *Spinidinium echinoideum* at 948,22 mbsf. However, the radiolarian studies suggest the beginning of the Turonian slightly upwards, where a typical association from the OAE 2 besides the FO of *Crucella cachensis* was recorded at 948,02 mbsf (Thurrow, 1988). This discrepancy also occurs when compared to the carbon isotope curve. The maximum values of $\delta^{13}\text{C}_{\text{org}}$ were recorded at 948,15 mbsf (Fig. 7), typically associated with the uppermost Cenomanian (Jarvis et al., 2011). Moreover, the FO of the radiolarian *C. cachensis* coincides with the extinction of the foraminifer genus *Rotalipora*, a common marker for the Cenomanian–Turonian boundary (Kuhnt et al., 1986). All these may suggest that the location of the Cenomanian–Turonian boundary would be at 948,02 mbsf as suggested by Thurrow (1988) instead of 948,22 mbsf suggested by the palynological data (Masure, 1984; this work). If the upper location of the Cenomanian–Turonian boundary is regarded, the FO of the dinoflagellate cyst *Dinogymnium cretaceum*, *Isabelidinium acuminatum*, and *Spinidinium echinoideum*, as well as the pollen *Trudopollis pertrudens*, would be slightly older than previously assumed (i.e., uppermost Cenomanian).

4.1.2. The OAE 2 in the Vigo Seamount

Several dark and fine organic-rich bed intervals were observed in core 398D-56 during DSDP Leg 47B in the late 1970s (Ryan et al.,

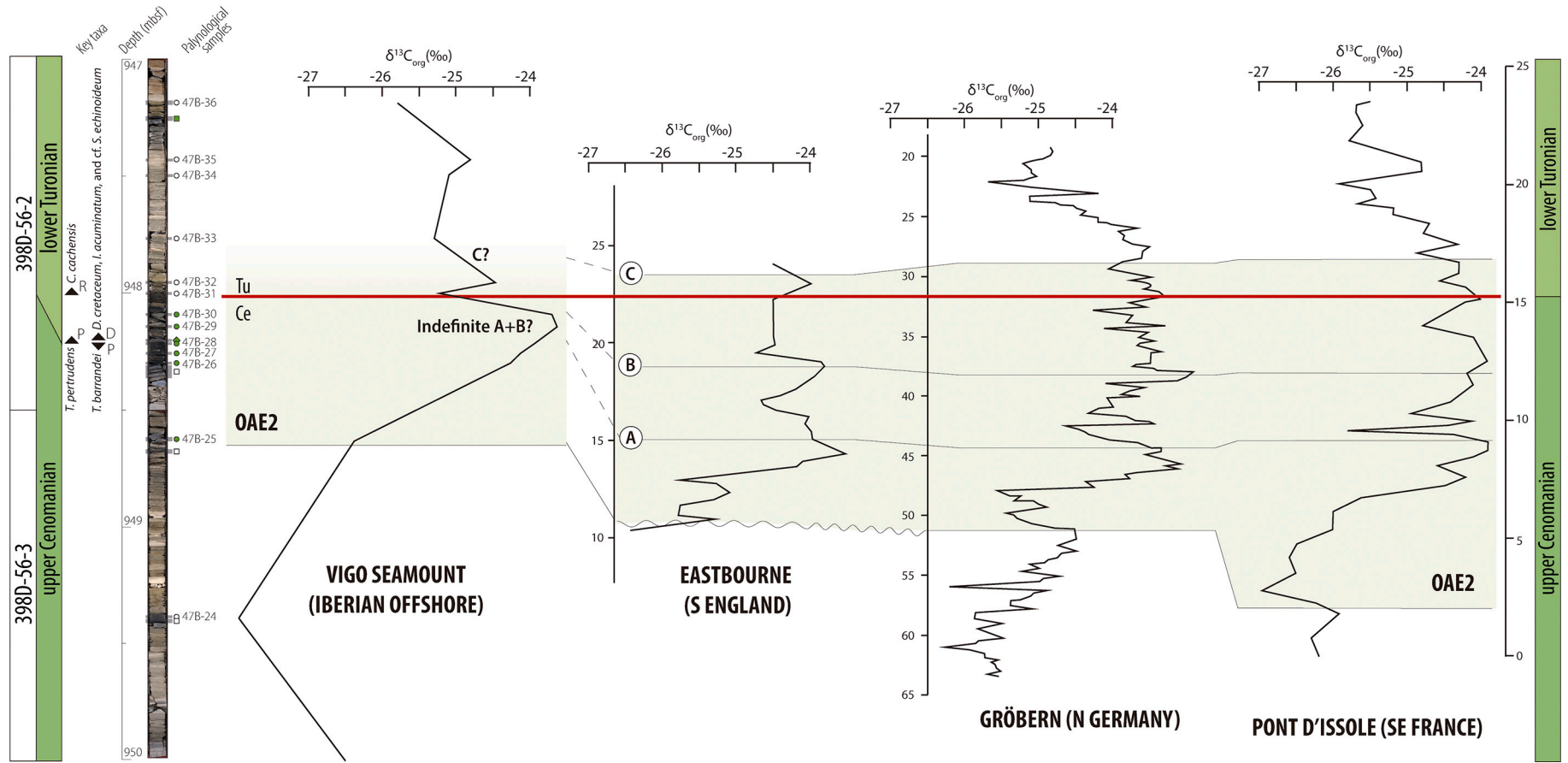


Fig. 7. Detailed section of the OAE 2 in the Vigo Seamount and $\delta^{13}\text{C}_{\text{org}}$ comparison to other European sections with significant expression of the OAE 2 (Jarvis et al., 2011). A–C are the three main $\delta^{13}\text{C}$ maxima. Abbreviation of biostratigraphic data: R, radiolarians; P, pollen; D, dinoflagellates. Palynological samples: square, Habib (1979a); diamond, Masare (1984); circle, this work; Filled in green, productive; filled in white, negative. (For interpretation of the references to colour in this figure legend, the reader is referred to the web version of this article.)

1979a). However, this was not recognized as the Cenomanian–Turonian OAE at the time. The definition of OAEs, including the OAE 2, improved in the 1980s (Jenkyns, 1980; Arthur et al., 1987) and further geochemical (Deroo et al., 1979; Arthur, 1979; Herbin et al., 1986) and biostratigraphical studies (Masure, 1984; Thurow et al., 1988) of Site 398 were undertaken. Therefore, some authors suggested that an expression of the OAE 2 may be present at Site 398 located between 947 and 949 mbsf (Herbin et al., 1986; Thurow et al., 1988).

Combined with the previously published biostratigraphic and geochemical data, we provide a new $\delta^{13}\text{C}_{\text{org}}$ record, which allows us to confirm the presence of the OAE 2. The OAE 2 interval begins at 948,60 while its upper limit is likely placed at 947,77 mbsf (Figs. 3 and 7). The top interval is an approximation due to data resolution. The OAE 2 sedimentary record at DSDP Site 398 is not characterized by a continuous black shale interval but by a section marked by an alternation of black shales with red and grey mudstones. According to the different stages for the OAE 2 proposed by Jarvis et al. (2011), the onset of the $\delta^{13}\text{C}$ positive excursion might correspond to the interval 948,60 to 948,10 mbsf, with the maximum levels of $\delta^{13}\text{C}$ at 948,15 mbsf (Fig. 7). The Plenus Cold Event (PCE) would apparently be located somewhere between 948,27 and 948,15 mbsf. However, condensation and lack of stratigraphic resolution hamper the identification of further OAE 2 stages.

Therefore, the local expression of the OAE 2 at DSDP Site 398 has the following characteristics: 1) it is represented by an alternation of grey and red mudstones with 5 to 10-cm thick intervals of thinly laminated and unburrowed dark mudstones (Thurow et al., 1988); 2) it begins at 948,60 mbsf and likely finishes at 948,77 mbsf, before the abrupt contact with the Plantagenet Formation; 3) it exhibits a 4‰ positive excursion in the $\delta^{13}\text{C}_{\text{org}}$, reaching a maximum value of -23.7‰ ; 4) it reaches a TOC of c. 10% which is mainly of marine origin (Deroo et al., 1979; Herbin et al., 1986); 5) the organic matter is a mixture of types II and III, where the uppermost OAE 2 deposits have hydrogen indices ranging between 200 and 380 mg HC/g TOC (Deroo et al., 1979; Herbin et al., 1986); 6) it has a low sedimentary rate of 1 m/Ma (Herbin et al., 1986).

4.2. Paleoenvironmental and paleoecological insights

A paleo-water depth of approximately 2000 m for Site 398 has been suggested from the Barremian up to the end of the Cretaceous, based on the dissolution of carbonated foraminiferal tests (Graciansky et al., 1978; Sigal, 1979). However, other authors suggest that the paleo-water depth of sedimentation could have been in a shallower environment. According to the palynological studies of Taugourdeau-Lantz et al. (1982), the presence of sporangia and immature spores suggests a shallower water environment with the existence of an emerged land-mass close to Site 398 during the Lower Cretaceous. The dissolution of the foraminiferal tests could also be explained by pore-water dissolution caused by CO_2 released during the anaerobic fermentation of organic matter in combination with humic acids. The relatively shallow water depth proposal was also supported by Masure (1984), who suggested that deposition of some stages (Aptian and Albian) may have occurred in an environment close to the coast in the neritic zone. Winterer et al. (1988) suggested, based on a combined seismic, lithological, and petrological analysis, that an emerged land mass must have been present at the Galicia Bank and other southward seamounts (including Vigo Seamount) between the Tithonian and the Aptian. However, by the Albian–Turonian interval, Site 398 would correspond to an open marine setting (or oceanic zone) consistent with the dinoflagellate community interpretation (see details below).

In most of the samples, the palynological content is highly dominated by continental palynomorphs in terms of diversity and abundance, with frequently good preservation. This does not necessarily exclude an environment located far away from the continent. The main drivers to transport continental palynological elements are surface runoff and

wind. In offshore environments, rivers are critical as a source of continental palynomorphs (Traverse, 1994; Hooghiemstra et al., 2006). Otherwise, the major wind belts will be the main transport driver (Hooghiemstra et al., 2006; Mudie and McCarthy, 2006). In both cases, terrestrial palynomorphs could be easily transported hundreds of kilometers from their continental source.

The ratio between the marine and continental fraction (PMI) in Site 398 remains stable through the studied section except for occasional peaks during the lower Cenomanian and a gradual drop in the upper Cenomanian–lower Turonian transition (Fig. 3). It is remarkable that slight variations in the PMI curve are often coincident with the P:G peaks (increased presence of heterotrophic dinoflagellates), and therefore may be linked to rising terrigenous input instead of sea-level variations. The presence of freshwater elements such as *Schizosporis* sp. seems to be transported together with the rest of the continental fraction.

The paleoecology of the marine elements is clearly dominated by Gonyaulacae taxa, but Areoligeraceae, Ceratiaceae, and Ovoidiniaceae are also well-represented (Fig. 8). The fossil genera *Pterodinium*, *Spiniferites*, and *Litosphaeridium* in the palynological assemblages A to C represent the dominant taxa. In addition to these taxa, Assemblage A contains a high abundance of *Circulodinium* and *Sepispinula*, which remains significant through Assemblage B for the case of *Sepispinula*. These three assemblages (A–C) are formed by an open marine community with oceanic conditions, regarding the dominance and presence of taxa restricted to this environment such as *Circulodinium colliveri*, *Cyclonephelium membraniphorum*, *Ellipsodinium rugulosum*, *Hystrichodinium pulchrum*, *Litosphaeridium siphoniphorum*, *Odontochitina operculata*, *Perosphaeridium cenomaniense*, and *Pterodinium cingulatum* (Harris and Tocher, 2003; Sánchez-Pellicer et al., 2018). The taxa mentioned above, together with other cosmopolitan taxa, like *Spiniferites* spp., represent the autochthonous elements. Other neritic taxa like *Oligosphaeridium pulcherrimum* (Sánchez-Pellicer et al., 2018), widely distributed in Hole 398D but never dominant in abundance, might be transported through surface currents from shallower environments. On the other hand, the generally low P:G ratio indicates a predominance of phototrophic taxa instead of heterotrophic ones, implying a low nutrient availability (Harland, 1973).

Remarkably, there is a pronounced decrease in the abundance and diversity of the marine elements around the OAE 2 (Fig. 3). This decline has two possible explanations: 1) the lack of preservation of the dinocysts and/or 2) the extinction of the autochthonous community of dinocysts. The former seems highly unlikely because the environment and depositional conditions are continuous, and the high abundance of other palynomorphs, like pollen, remains stable. The presence of a few dinoflagellate cysts, with their first record in Site 398 around the OAE 2, such as *Canningia reticulata* or *Gardodinium* sp., could be indicative of an extinction of the autochthonous community and the first stages of a turnover during the OAE 2 at the Vigo Seamount.

As mentioned before, the continental palynomorphs are well represented in Hole 398D. Their main source is possibly the Iberian Peninsula, as the Galicia Hills were submerged by the late Albian–Cenomanian (Winterer et al., 1988). The palynological content of offshore sediments still represents the onshore plant communities, as shown in palynological studies from recent offshore sediments compared with the onshore plant pattern distributions (e.g., Hooghiemstra et al., 2006). However, these values should be used carefully and treated as qualitative data, as the distribution of offshore sediments and (consequently) palynomorphs is primarily affected by transport and sedimentation processes (Traverse, 1994). After these considerations, an approximation of the land vegetation in NW Iberia has been reconstructed for the studied interval (Fig. 8).

Based on the Hole 398D palynological record, plant communities between the latest Albian and the middle Cenomanian were apparently dominated by three groups with changing contribution: pteridophytes (mainly Anemiaceae and Cyatheaceae), Pinaceae–Podocarpaceae conifers, and Cheirolepidiaceae conifers. Their dominance was more or

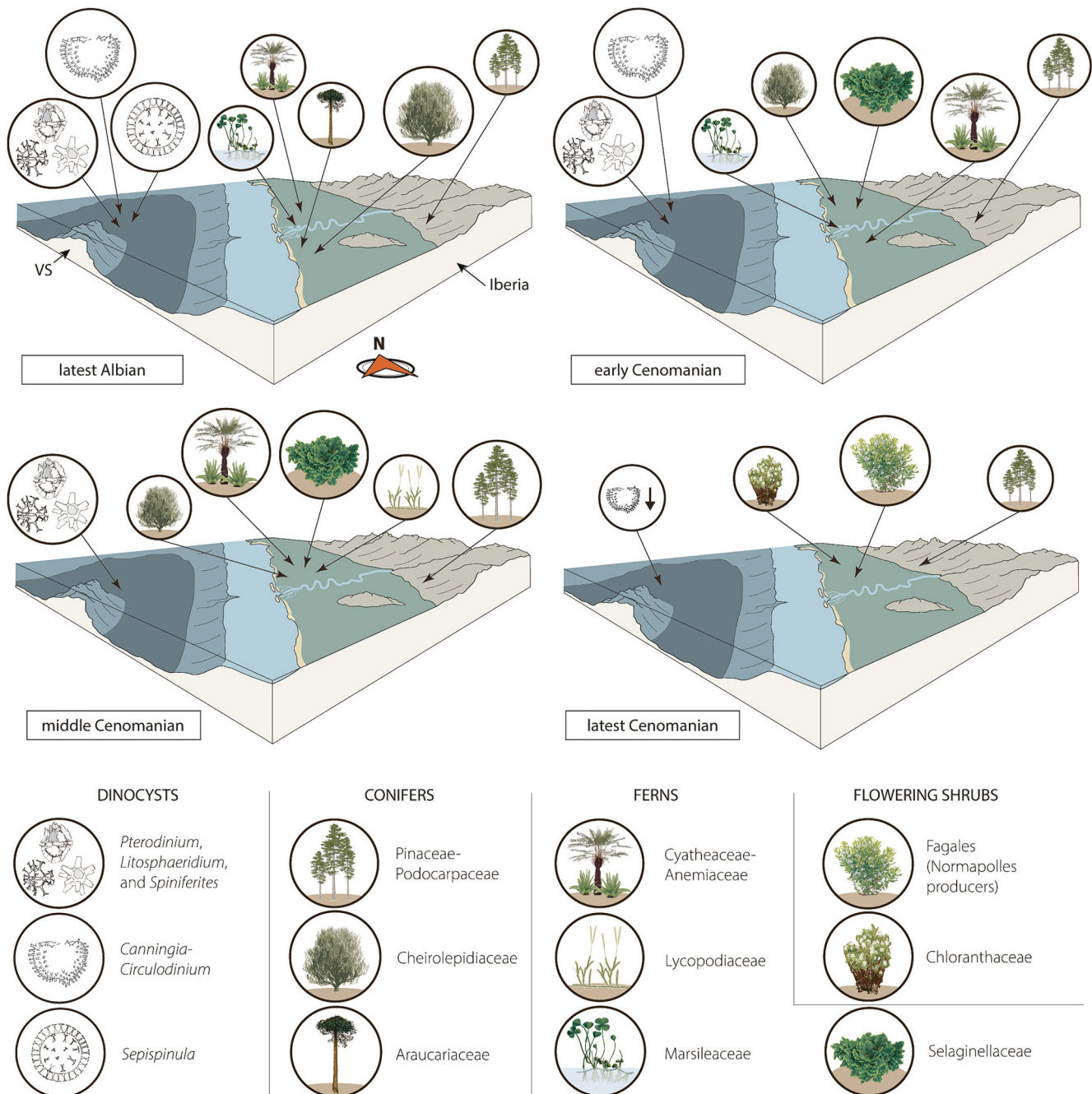


Fig. 8. Paleocological reconstruction of marine and continental communities during four different intervals within the latest Albian to Cenomanian period. Size of the circles indicate more or less predominance. VS: Vigo Seamount.

less stable during the Early Cretaceous and marked a clear difference from the Late Jurassic and Jurassic–Cretaceous boundary floras of Iberia (e.g., Rodríguez-Barreiro et al., 2022; Santos et al., 2018, 2022a, 2022b).

The pteridophyte group varies in abundance and diversity, but was present in all reconstructed plant communities, probably as a main component in the understory vegetation formed by herbaceous and arborescent ferns related to more humid conditions. The families contributing most to this group were Cyatheaceae and Schizaeales (putative Anemiaceae). However, in assemblages A and B, the aquatic fern Marsileaceae was also highly represented, suggesting the presence of freshwater ponds or shallow lakes (Smith et al., 2006). Other families, such as Lycopodiaceae and Gleicheniaceae, were also significantly present in assemblages B and C.

In contrast, the abundance of the Pinaceae-Podocarpaceae conifer group is relatively low but remains constant throughout the studied section. This group would have formed the canopy in the plant community with tall, woody trees. The Cheirolepidiaceae formed the intermediate part of this community with medium-sized conifers. This group is dominant only in the 965,0–965,83 mbsf interval within Assemblage A (Fig. 3). Plants of the Cheirolepidiaceae family were thermophilic and adapted to a wide range of environments, but several species indicate a preference for coastal and semi-arid environments (Alvin, 1982; Watson and Alvin, 1996). Its presence in high relative abundance (>50%) is characteristic of low latitudes (i.e., lower than 40°; Vakhrameev, 1970). These high proportions indicate an increase in the global temperatures and aridity during a relatively short period on land associated with a rise in sea surface temperatures in the latest Albian, prior to a cooling phase

in the Albian–Cenomanian boundary (Forster et al., 2007). This short warm period during the latest Albian may have favored the spread of forests dominated by Cheirolepidiaceae towards northern latitudes.

One of the major floral turnovers was observed during the late Cenomanian–early Turonian. During this time, the plant communities became dominated by angiosperms, specifically from the Normapolles group. This change occurs right at the beginning of the OAE 2 (948,60 mbsf upwards). This group is related to the Fagales (Batten, 1981; Friis et al., 2006). The living conditions of the earlier representatives of this order are still uncertain. Many different environments have been proposed for the Normapolles-producing plants, including uplands (Lubir-omova and Samoilovich, 1975) or mangroves (Paclová, 1978). They seem to have been a heterogeneous group adapted to both humid and arid environments (Zaklinskaya, 1977; Batten, 1984), and the first Normapolles parent plants were small non-woody shrubs forming open low-density forests in seasonally variable conditions (Batten, 1984; Philippe et al., 2008; Heimhofer et al., 2018). Therefore, during the late Cenomanian–early Turonian time interval, the onshore plant community close to the Vigo Seamount could be described as an open woodland dominated mainly by Normapolles-producing shrubs.

4.3. Palynological response to the OAE 2

4.3.1. Marine palynological response

Regarding marine palynomorphs, our results reveal a distinct decline in both the abundance and diversity of the dinoflagellate cysts (Fig. 3), which seems unrelated to preservation. This extinction initiates with the onset of the OAE 2, at 948,60 mbsf, and intensifies notably during the $\delta^{13}\text{C}$ positive peak. It should be noted the presence of an earlier declining trend in diversity and dinocysts abundance (Fig. 3), apparently suggesting a decline preceding the OAE 2. However, it is important to recognize the effect of barren sample 47B-24, at 949,37 mbsf, which introduces a ‘false’ earlier declining trend in the diagrams (Fig. 3). Regardless of the graphical representation, our data indicates a 30% decrease in relative abundance and an 80% reduction in the diversity of the dinocysts fossil genera between pre-OAE 2 and OAE 2 levels. Similar trends have been observed in nearby locations (i.e., the Galicia Bank), with a 70% decrease in fossil genera during the OAE 2 (Thurrow et al., 1988).

Closer to the coast, in the Eastern proto-North Atlantic neritic environments, the environmental changes during the OAE 2 are mainly reflected in sea-level and sea surface temperature variations (Pearce et al., 2009). According to these authors, a productivity pulse showing an increased abundance of dinoflagellate cysts during the Plenus Cold Event (PCE) was detected prior to the $\delta^{13}\text{C}$ positive excursion, followed by a biotic crisis (in abundance and diversity) after the PCE and an eventual recovery in the later early Turonian.

In the Western proto-North Atlantic, a turnover of the marine palynological assemblages seems to occur around the OAE 2 (Habib, 1972; Habib and Drugg, 1987; Herbin et al., 1987). Indeed, a detailed study of the OAE 2 palynology from the Cretaceous Western Interior Seaway differentiated the following phases (Dodsworth and Eldrett, 2019): 1) a slight decrease of the relative abundance of dinocysts in the first half of the OAE 2, 2) a decrease in diversity in the interval corresponding to the PCE identified in the Pueblo section as the ‘benthic oxic zone’ (Keller and Pardo, 2004), and 3) a consistent presence of boreal dinocysts (i.e., *Cyclonephelium compactum-membraniphorum*; van Helmond et al., 2016) during and after the PCE.

In the palynological studies from the OAE 2 of the Iberian Peninsula, the difference between assemblages seems to be controlled by their paleogeographical location, while no major extinctions have been observed (Lamolda and Mao, 1999; Peyrot et al., 2011, 2012). However, in the Castilian Platform (N Spain), a slight decrease in the relative abundance during the OAE 2 was observed (Lamolda and Mao, 1999), with a remarkable boreal influence in terms of abundance (Peyrot et al., 2011, 2012), probably corresponding to the PCE.

Perturbations in dinoflagellate marine communities during the OAE 2 are evident, marked by a decrease in relative abundance and diversity, along with an incursion of boreal elements during cooling phases. However, the significance of each factor appears to vary, contingent on the specific marine environment. In the NW Iberia offshore, a decline in dinocyst relative abundance and diversity is observed exclusively. This area represents an open marine paleoenvironment with low nutrient conditions, as confirmed by the P:G ratio (Fig. 3), yielding a low diversity community where biotic changes may manifest subtly. In addition, a sedimentological condensation is present in the OAE 2 interval. Consequently, the interpretation could not extend beyond identifying an OAE 2-related extinction in the NW Iberia offshore, aligning with previous findings from other studies.

4.3.2. Terrestrial palynological response

In the continental palynoflora, an evident change occurs during the OAE 2. The diversification and dominance of the Normapolles-group pollen are significant. The dominance peak of this group is almost coincident with the $\delta^{13}\text{C}_{\text{org}}$ positive excursion (Fig. 3). Moreover, the diversification of the Normapolles pollen becomes relevant and appears to proceed rapidly from the first occurrence of a Normapolles pollen (i.e., *Complexiopollis* sp.) in the middle Cenomanian (average of two fossil species) to the upper Cenomanian (average of 10 fossil species), and the OAE 2 interval (average of 13 fossil species).

This event is not exclusively documented from Hole 398D. A similar peak of dominance, combined with a rapid diversification of this group, was also observed at the OAE 2 of the adjacent DSDP Site 641 (Leg 103) on the Galicia Bank (Thurrow et al., 1988). In other nearby areas, such as northern Spain (Peyrot et al., 2008) and southeastern France (Heimhofer et al., 2018), a lower-scale Normapolles dominance was also identified. However, these changes were not ubiquitous during the OAE 2, as they were not observed in other microfloras from Portugal or France (e.g., Groot and Groot, 1962; Svobodová et al., 1998; Méon et al., 2004). On the other side of the proto-Atlantic, Normapolles angiosperms were also a relevant element of the floras from NE America. In the New Jersey coast, a presumably early Normapolles-dominant microflora was identified within the Raritan Fm. (Christopher, 1979). However, with a suggested middle–upper Cenomanian age for these deposits, a lower Turonian is not excluded by several authors (Wolfe and Pakiser, 1971; Doyle and Robbins, 1977), lacking correlation to the OAE 2.

Although the anemophilous dispersion attributed to the Normapolles (Doyle and Hickey, 1976; Friis et al., 2011) may result in their overrepresentation in marine deposits, Normapolles-producers were a significant part of the plant communities during the OAE 2 on the margins of the proto-North Atlantic. The climatic changes during the Cenomanian–Turonian interval, which resulted in the OAE 2, may have had an effect on the spreading of this botanical group. For example, Heimhofer et al. (2018) suggest that the cooler and drier conditions of the PCE within the OAE 2 favored the proliferation of the Normapolles in mid-latitude locations and, once established, they were able to persist during warmer conditions. However, our data suggests that the diversification of the Normapolles began before the PCE, during the onset of the $\delta^{13}\text{C}$, somewhere between 948,60 and 949,37 mbsf. At the beginning of the OAE 2, the Normapolles were already dominant, with >60% of relative abundance. According to the terrigenous sediment source for Hole 398D as northern Iberia, along with other early Normapolles-dominant assemblages from the same region, differences in Normapolles radiation timing throughout the late Cenomanian were paleogeographically-dependent, likely due to regional climate variations.

5. Conclusions

The combined palynological and geochemical study confirmed the presence of the OAE 2 in Site 398, in the interval between 949,60 and 947,25 mbsf, according to the $\delta^{13}\text{C}_{\text{org}}$ isotope analysis. Moreover, four

palynological assemblages were differentiated, corresponding to an upper Albian (A), lower Cenomanian (B), middle Cenomanian (C), and upper Cenomanian–lower Turonian (D). The detailed palynological dating enhanced the age assignment of the uppermost part of the Hateras Fm. in Hole 398D.

The marine community represented in the palynological assemblages was usually dominated by Gonyaulacaceae and, to a lesser extent, Areoligeraceae dinoflagellate cysts, such as *Pterodinium*, *Circulodinium*, *Litospheeridium*, *Sepispinula*, and *Spiniferites*, depending on the assemblage. The terrestrial plant community of the late Albian to middle Cenomanian interval was commonly dominated by three groups: Pinaceae–Podocarpaceae conifers, Cheirolepidiaceae conifers, and Anemiaceae–Cyatheaceae pteridophytes. During the late Cenomanian to early Turonian interval (particularly during the OAE 2), the Normapolles angiosperms became the dominant group of the continental plant communities.

Associated with the OAE 2, two major turnovers were observed. A decrease in diversity and abundance of dinoflagellate cysts and, in the terrestrial plant community, a rapid diversification and increase in the relative dominance of the Normapolles pollen were observed. The abundance peak of Normapolles almost parallels the $\delta^{13}\text{C}$ positive excursion.

CRediT authorship contribution statement

Iván Rodríguez-Barreiro: Conceptualization, Data curation, Formal analysis, Investigation, Methodology, Visualization, Writing – original draft. **Artai A. Santos:** Conceptualization, Investigation, Writing – review & editing. **Uxue Villanueva-Amadoz:** Investigation, Supervision, Validation, Writing – review & editing. **Stephen Louwye:** Investigation, Resources, Writing – review & editing, Formal analysis. **Stuart A. Robinson:** Formal analysis, Investigation, Methodology, Writing – review & editing. **José B. Diez:** Conceptualization, Funding acquisition, Supervision, Writing – review & editing.

Declaration of competing interest

The authors declare that they have no known competing financial interests or personal relationships that could have appeared to influence the work reported in this paper.

Data availability

Data available within the supplementary materials.

Acknowledgments

The authors are grateful to the Bremen Core Repository for providing the sample material used to carry out this study. We also appreciate the services provided by the CACTI for Scanning Electron Microscopy and IRMS analysis. Funding for this research was provided by the Xunta de Galicia (Spain), through project EDC431C-2019/28. IRB was supported by a predoctoral fellowship from the Xunta de Galicia (Spain) and the European Social Fund-European Union (ref.: ED481A-2020/175). AAS was supported by a postdoctoral fellowship from the Swedish Research Council Grant (VR 2022-03920) managed by Dr. Stephen McLoughlin. We gratefully acknowledge the constructive suggestions of the editor Dr. Bing Shen, as well as Dr. Elke Schneebeil and other three anonymous reviewers. Funding for open access charge: Universidade de Vigo/ CISUG.

Appendix A. Supplementary data

Supplementary data to this article can be found online at <https://doi.org/10.1016/j.palaeo.2024.112223>.

References

- Alves, T.M., Moita, C., Cunha, T., Ullnaess, M., Myklebust, R., Monteiro, J.H., Manuppella, G., 2009. Diachronous evolution of Late Jurassic–Cretaceous continental rifting in the northeast Atlantic (west Iberian margin). *Tectonics* 28 (4). <https://doi.org/10.1029/2008TC002337>.
- Alvin, K.L., 1982. Cheirolepidiaceae: biology, structure and paleoecology. *Rev. Palaeobot. Palynol.* 37 (1–2), 71–98. [https://doi.org/10.1016/0034-6667\(82\)90038-0](https://doi.org/10.1016/0034-6667(82)90038-0).
- Antonescu, E., 1973. Asociatii palinologice caracteristice unor formatiuni Cretacee din Muntii Metaliferi. *Dari de Seama al Şedintelor* 59 (3), 115–169.
- Arthur, M.A., 1979. North Atlantic cretaceous black shales: the record at Site 398 and a brief comparison with other occurrences. *Initial Rep. Deep Sea Drill. Proj.* 47 (2), 719–751. <https://doi.org/10.2973/dsdp.proc.47-2.116.1979>.
- Arthur, M.A., Scholle, P.A., Hasson, P., 1979. Stable isotopes of oxygen and carbon in carbonates from Sites 398 and 116 of the Deep Sea Drilling Project. *Initial Rep. Deep Sea Drill. Proj.* 47 (2), 477–492. <https://doi.org/10.2973/dsdp.proc.47-2.114.1979>.
- Arthur, M.A., Schlanger, S.O., Jenkyns, H.C., 1987. The Cenomanian–Turonian Oceanic Anoxic Event II. *Paleoceanographic controls on organic matter production and preservation*. In: Brooks, J., Fleet, A. (Eds.), *Marine Petroleum Source Rocks*. Geological Society London Special Publication, London, UK, pp. 401–420.
- Azéma, C., Fauconnier, D., Viaud, J.M., 1981. Microfossils from the upper cretaceous of Vendée (France). *Rev. Palaeobot. Palynol.* 35 (2–4), 237–281. [https://doi.org/10.1016/0034-6667\(81\)90111-1](https://doi.org/10.1016/0034-6667(81)90111-1).
- Azéma, C., Fauconnier, D., Neumann, M., 1990. Apport de données palynologiques à l'étude du Cénomanién de part et d'autre du seuil du Poitou (France). *Rev. Micropaleontol.* 33 (1), 3–23.
- Barclay, R.S., McElwain, J.C., Sageman, B.B., 2010. Carbon sequestration activated by a volcanic CO₂ pulse during Ocean Anoxic Event 2. *Nat. Geosci.* 3 (3), 205–208. <https://doi.org/10.1038/ngeo757>.
- Barron, E.J., Fawcett, P.J., Peterson, W.H., Pollard, D., Thompson, S.L., 1995. A “simulation” of mid-Cretaceous climate. *Paleoceanography* 10 (5), 953–962. <https://doi.org/10.1029/95PA01624>.
- Batten, D.J., 1981. Stratigraphic, palaeogeographic and evolutionary significance of Late Cretaceous and early Tertiary Normapolles pollen. *Rev. Palaeobot. Palynol.* 35 (2–4), 125–137. [https://doi.org/10.1016/0034-6667\(81\)90104-4](https://doi.org/10.1016/0034-6667(81)90104-4).
- Batten, D.J., 1984. Palynology, climate and the development of Late Cretaceous floral provinces in the Northern Hemisphere: a review. In: Brenchley, P. (Ed.), *Fossils and Climate*. John Wiley & Sons, Ltd, pp. 127–164.
- Batten, D.J., Marshall, K.L., 1991. Palynology of Upper Cretaceous “Black Shales” from Helgoland, South North Sea. In: Schmid, F., Spaeth, C. (Eds.), *The Cretaceous of the North Sea, Helgoland*. Geologisches Jahrbuch Reihe A, pp. 105–115.
- Bleischmidt, G., 1979. Biostratigraphy of calcareous nannofossils: Leg 47B, deep sea drilling project. *Initial Rep. Deep Sea Drill. Proj.* 47 (2), 327–360. <https://doi.org/10.2973/dsdp.proc.47-2.106.1979>.
- Boudinot, F.G., Kopf, S., Dildar, N., Sepúlveda, J., 2021. Carbon cycling during oceanic anoxic event 2: compound-specific carbon isotope evidence from the western interior seaway. *Paleoceanogr. Paleoclimatol.* 36 (9), e2021PA004287 <https://doi.org/10.1029/2021PA004287>.
- Boullia, S., Charbonnier, G., Spangenberg, J.E., Gardin, S., Galbrun, B., Briard, J., Le Callonnec, L., 2020. Unraveling short- and long-term carbon cycle variations during the Oceanic Anoxic Event 2 from the Paris Basin Chalk. *Global Planet. Change* 186, 103126. <https://doi.org/10.1016/j.gloplacha.2020.103126>.
- Chamley, H., Debrabant, P., Foulon, J., d'Argoud, G.G., Latouche, C., Maillot, N., Sommer, F., 1979. Mineralogy and geochemistry of cretaceous and Cenozoic Atlantic sediments off the Iberian peninsula (Site 398, DSDP Leg 47B). *Initial Rep. Deep Sea Drill. Proj.* 47 (2), 429–449. <https://doi.org/10.2973/dsdp.proc.47-2.111.1979>.
- Christopher, R.A., 1977. Selected normapolles pollen genera and the age of the Raritan and Magothy Formations (Upper Cretaceous) of northern New Jersey. In: Owens, J. P., Minard, J.P., Sohl, N.F. (Eds.), *A field guide to Cretaceous and lower Tertiary beds of the Raritan and Salisbury embayments, New Jersey, Delaware, and Maryland: Guidebook prepared for the annual AAPG/SEPM convention*. American Association of Petroleum Geologists—Society of Economic Paleontologists and Mineralogists, Washington, DC, pp. 58–69.
- Christopher, R.A., 1979. Normapolles and triporate pollen assemblages from the Raritan and Magothy Formations (Upper Cretaceous) of New Jersey. *Palynology* 3 (1), 73–121. <https://doi.org/10.1080/01916122.1979.9989185>.
- Deroo, G., Herbin, J.P., Roucaché, J., Tissot, B., 1979. Organic geochemistry of Cretaceous shales from DSDP site 398, leg 47B, eastern North Atlantic. *Initial Rep. Deep Sea Drill. Proj.* 47 (2), 513–522. <https://doi.org/10.2973/dsdp.proc.47-2.118.1979>.
- Dodsworth, P., Eldrett, J.S., 2019. A dinoflagellate cyst zonation of the Cenomanian and Turonian (Upper Cretaceous) in the Western Interior, United States. *Palynology* 43 (4), 701–723. <https://doi.org/10.1080/01916122.2018.1477851>.
- Doyle, J.A., Hickey, L.J., 1976. Pollen and leaves from the mid-Cretaceous Potomac Group and their bearing on early angiosperm evolution. In: Beck, C.B. (Ed.), *Origin and Early Evolution of Angiosperms*. Columbia University Press, New York, NY, pp. 139–206.
- Doyle, J.A., Robbins, E.I., 1977. Angiosperm pollen zonation of the continental cretaceous of the Atlantic coastal plain and its application to deep wells in the Salisbury embayment. *Palynology* 1 (1), 41–78. <https://doi.org/10.1080/01916122.1977.9989150>.
- Duxbury, S., 2001. A palynological zonation scheme for the Lower Cretaceous–United Kingdom sector, central North Sea. *Neues Jahrbuch Für Geologie Und Paläontologie-Abhandlungen* 219 (1–2), 95–137. <https://doi.org/10.1127/njgpa/219/2001/95>.

- Fauconnier, D., 1975. Répartition des Peridiniens de l'Albien du Bassin de Paris Role stratigraphique et Liaison avec le Cadre sedimentologique. *Bulletin du Bureau des Recherches Géologiques et Minières (Deuxième serie)* 1 (4), 235–273.
- Fechner, G.G., Dargel, C., 1989. Die Cenoman-Ablagerungen Nördlich von Simeyrols (Dept. Dordogne, SW-Frankreich): Sedimentologie, Paläontologie, Palynologie. *Berliner Geowissenschaftliche Abhandlungen, Reihe A, Geologie und Paläontologie* 106, 73–97.
- Fensome, R.A., Taylor, F.J.R., Norris, G., Sarjeant, W.A.S., Wharton, D.I., Williams, G.L., 1993. A classification of fossil and living dinoflagellates. *Micropaleontology Press Special Paper* 7, 1–351.
- Fischer, V., Bardet, N., Benson, R.B., Arkhangelsky, M.S., Friedman, M., 2016. Extinction of fish-shaped marine reptiles associated with reduced evolutionary rates and global environmental volatility. *Nat. Commun.* 7, 10825 <https://doi.org/10.1038/ncomms10825>.
- Folli, K.B., 1995. 160 my record of marine sedimentary phosphorus burial – coupling of climate and continental weathering under Greenhouse and Icehouse conditions. *Geology* 23 (9), 859–862. [https://doi.org/10.1130/0091-7613\(1995\)023<0503:MYROMS>2.3.CO;2](https://doi.org/10.1130/0091-7613(1995)023<0503:MYROMS>2.3.CO;2).
- Forster, A., Schouten, S., Baas, M., Sinninghe Damsté, J.S., 2007. Mid-Cretaceous (Albian–Santonian) sea surface temperature record of the tropical Atlantic Ocean. *Geology* 35 (10), 919–922. <https://doi.org/10.1130/G23874A.1>.
- Freeman, K.H., Hayes, J.M., 1992. Fractionation of carbon isotopes by phytoplankton and estimates of ancient CO₂ levels. *Global Biogeochem. Cycles* 6 (2), 185–198. <https://doi.org/10.1029/92GB00190>.
- Friis, E.M., Pedersen, K.R., Schönenberger, J., 2006. Normapolles plants: a prominent component of the Cretaceous rosoid diversification. *Plant Syst. Evol.* 260 (2), 107–140. <https://doi.org/10.1007/s00606-006-0440-y>.
- Friis, E.M., Crane, P.R., Pedersen, K.R. (Eds.), 2011. *Early Flowers and Angiosperm Evolution*. Cambridge University Press, Cambridge, UK.
- Galasso, F., Heimhofer, U., Schneebeli-Hermann, E., 2023. The Cenomanian/Turonian boundary in light of new developments in terrestrial palynology. *Sci. Rep.* 13 (1), 3074. <https://doi.org/10.1038/s41598-023-30072-6>.
- Gangl, S.K., Moy, C.M., Stirling, C.H., Jenkyns, H.C., Crampton, J.S., Clarkson, M.O., Ohneiser, C., Porcelli, D., 2019. High-resolution records of Oceanic Anoxic Event 2: Insights into the timing, duration and extent of environmental perturbations from the palaeo-South Pacific Ocean. *Earth Planet. Sci. Lett.* 518, 172–182. <https://doi.org/10.1016/j.epsl.2019.04.028>.
- Graciansky, P.D., Chenet, P.Y., 1979. Sedimentological study of Cores 138 to 56 (upper Hauterivian to middle Cenomanian): an attempt at reconstruction of paleoenvironments. *Initial Rep. Deep Sea Drill. Proj.* 47 (2), 403–418. <https://doi.org/10.2973/dsdp.proc.47-2.109.1979>.
- Graciansky, P.C., Muller, C., Rehault, J.P., Sigal, J., 1978. Reconstitution de l'évolution des milieux de sédimentation sur la marge continentale ibérique au Crétacé: le flanc sud du haut-fond de Vigo et le forage DSDP-IPOD 398D; problèmes concernant la surface de compensation des carbonates. *Bulletin de la Société Géologique de France* 7 (4), 389–399.
- Groot, J.J., Groot, C.R., 1962. Plant microfossils from Aptian, Albian and Cenomanian deposits of Portugal. *Comunicações dos Serviços Geológicos de Portugal* 46, 133–176.
- Habib, D., 1972. Dinoflagellates and other palynomorphs in selected samples from Leg 14, Deep Sea Drilling Project. *Initial Rep. Deep Sea Drill. Proj.* 14, 649–653. <https://doi.org/10.2973/dsdp.proc.14.117.1972>.
- Habib, D., 1979a. Sedimentology of palynomorphs and palynodebris in Cretaceous carbonaceous facies south of Vigo Seamount. *Initial Rep. Deep Sea Drill. Proj.* 47 (2), 451–465. <https://doi.org/10.2973/dsdp.proc.47-2.112.1979>.
- Habib, D., 1979b. Sedimentary origin of North Atlantic Cretaceous palynofacies. In: *Deep Drilling Results in the Atlantic Ocean: Continental Margins and Paleoenvironment*, 3, pp. 420–437. <https://doi.org/10.1029/ME003p0420>.
- Habib, D., Drugg, W.S., 1987. Palynology of sites 603 and 605, Leg 93, Deep Sea Drilling Project. *Initial Rep. Deep Sea Drill. Proj.* 93, 751–775. <https://doi.org/10.2973/dsdp.proc.93.122.1987>.
- Hag, B.U., 2014. Cretaceous eustasy revisited. *Global Planet. Change* 113, 44–58. <https://doi.org/10.1016/j.gloplacha.2013.12.007>.
- Harland, R., 1973. Dinoflagellate cysts and acritarchs from the Bearpaw Formation (Upper Campanian) of southern Alberta, Canada. *Palaeontology* 16, 665–706.
- Harris, A.J., Tocher, B.A., 2003. Palaeoenvironmental analysis of Late Cretaceous dinoflagellate cyst assemblages using high-resolution sample correlation from the Western Interior Basin, USA. *Mar. Micropaleontol.* 48 (1–2), 127–148. [https://doi.org/10.1016/s0377-8398\(03\)00002-1](https://doi.org/10.1016/s0377-8398(03)00002-1).
- Heimhofer, U., Wucherpfennig, N., Adatte, T., Schouten, S., Schneebeli-Hermann, E., Gardin, K.G., Kentsch, S., Kujau, A., 2018. Vegetation response to exceptional global warmth during Oceanic Anoxic Event 2. *Nat. Commun.* 9 (1), 1–8. <https://doi.org/10.1038/s41467-018-06319-6>.
- Helenes, J., de Guerra, C., Vázquez, J., 1998. Palynology and chronostratigraphy of the Upper Cretaceous in the subsurface of the Barinas area, western Venezuela. *Am. Assoc. Pet. Geol. Bull.* 82, 1308–1328. <https://doi.org/10.1306/1D9BCA61-172D-11D7-8645000102C1865D>.
- Herbin, J.P., Montadert, L., Muller, C., Gomez, R., Thurow, J., Wiedmann, J., 1986. Organic-rich sedimentation at the Cenomanian–Turonian Boundary in oceanic and coastal basins in the North Atlantic and Tethys. In: Summerhayes, C.P., Shackleton, N.J. (Eds.), *North Atlantic Palaeoceanography*. Geological Society Special Publications, London, UK, pp. 389–422.
- Herbin, J.P., Masure, E., Roucach, J., 1987. Cretaceous formations from the lower continental rise off Cape Hatteras: organic geochemistry, dinoflagellate cysts, and the Cenomanian/Turonian boundary event at sites 603 (Leg 93) and 105 (Leg 11). *Initial Rep. Deep Sea Drill. Proj.* 93, 1139–1162. <https://doi.org/10.2973/dsdp.proc.93.147.1987>.
- Herngreen, G.F.W., Chlonova, A.F., 1981. Cretaceous microfossil provinces. *Pollen Spores* 23 (3), 441–555.
- Hochuli, P.A., 1981. North Gondwanan floral elements in lower to middle Cretaceous sediments of the southern Alps (southern Switzerland, northern Italy). *Rev. Palaeobot. Palynol.* 35 (2–4), 337–358. [https://doi.org/10.1016/0034-6667\(81\)90116-0](https://doi.org/10.1016/0034-6667(81)90116-0).
- Hong, S.K., Lee, Y.I., 2012. Evaluation of atmospheric carbon dioxide concentrations during the Cretaceous. *Earth Planet. Sci. Lett.* 327–328, 23–28. <https://doi.org/10.1016/j.epsl.2012.01.014>.
- Hooghiemstra, H., Lézine, A.M., Leroy, S.A., Dupont, L., Marret, F., 2006. Late Quaternary palynology in marine sediments: a synthesis of the understanding of pollen distribution patterns in the NW African setting. *Quat. Int.* 148 (1), 29–44. <https://doi.org/10.1016/j.quaint.2005.11.005>.
- Huber, B.T., Norris, R.D., MacLeod, K.G., 2002. Deep-sea paleotemperature record of extreme warmth during the Cretaceous. *Geology* 30 (2), 123–126. [https://doi.org/10.1130/0091-7613\(2002\)030<0123:DSPROE>2.0.CO;2](https://doi.org/10.1130/0091-7613(2002)030<0123:DSPROE>2.0.CO;2).
- Ibrahim, M.I., Tahoun, S.S., Zobia, M.K., Obok-Ikuenobe, F.E., Kholeif, S.E., 2020. Late Cretaceous palynology and paleoenvironment of the Razzak-3 well, north Western Desert, Egypt. *Arab. J. Geosci.* 13 (17), 1–23. <https://doi.org/10.1007/s12517-020-05705-z>.
- Jarvis, I., Lignum, J.S., Gröcke, D.R., Jenkyns, H.C., Pearce, M.A., 2011. Black shale deposition, atmospheric CO₂ drawdown, and cooling during the Cenomanian–Turonian Oceanic Anoxic Event. *Paleoceanography* 26, PA3201. <https://doi.org/10.1029/2010PA002081>.
- Jenkyns, H.C., 1980. Cretaceous anoxic events: from continents to oceans. *J. Geol. Soc. London* 137, 171–188. <https://doi.org/10.1144/gsjgs.137.2.0171>.
- Jenkyns, H.C., 2010. Geochemistry of oceanic anoxic events. *Geochem. Geophys. Geosyst.* 11 (3) <https://doi.org/10.1029/2009GC002788>.
- Jenkyns, H.C., Gale, A.S., Corfield, R.M., 1994. Carbon- and oxygen-isotope stratigraphy of the English Chalk and Italian Scaglia and its palaeoclimatic significance. *Geol. Mag.* 131, 1–34. <https://doi.org/10.1017/S001675800010451>.
- Kedves, M., 1980. Les pollens du genre de forme *Complexipollis* W. Kr. 1959 em. *Tschudy 1973 du Cénomanien Supérieur de Vila Flor (Portugal)*. *Rev. Esp. Micropaleontol.* 12, 469–488.
- Kedves, M., Diniz, F., 1979. Les pollens d'Angiospermes du Crétacé de Vila Flor, Portugal. *Genres de Forme Atlantipollis et Limaipollenites*. *Boletim da Sociedade Geologica de Portugal* 21, 203–216.
- Keller, G., Pardo, A., 2004. Age and paleoenvironment of the Cenomanian–Turonian global stratotype section and point at Pueblo, Colorado. *Mar. Micropaleontol.* 51 (1–2), 95–128. <https://doi.org/10.1016/j.marmicro.2003.08.004>.
- Kennedy, W.J., Gale, A.S., Lees, J.A., Caron, M., 2004. The global boundary stratotype section and point (GSSP) for the base of the Cenomanian Stage, Mont Risou, Hautes-Alpes, France. *Episodes J. Int. Geosci.* 27 (1), 21–32. <https://doi.org/10.18814/epiugs/2004/v27i1/003>.
- Kerr, A.C., 1998. Oceanic plateau formation: a cause of mass extinction and black shale deposition around the Cenomanian–Turonian boundary? *J. Geol. Soc. London* 155 (4), 619–626. <https://doi.org/10.1144/gsjgs.155.4.061>.
- Kimyai, A., 1966. Palynology of the Raritan Formation (Cretaceous) in New Jersey. *Micropaleontology* 12 (4), 461–476. <https://doi.org/10.2307/1484790>.
- Kimyai, A., 1970. Plant microfossils from the Raritan Formation (Cretaceous) in Long Island. *Pollen Spores* 12, 181–204.
- Kuhnt, W., Thurow, J., Wiedmann, J., Herbin, J.-P., 1986. Oceanic anoxic conditions around the Cenomanian/Turonian Boundary and the response of the biota. In: Degens, E.T., Meyers, P.A., Brassell, S.C. (Eds.), *Biogeochemistry of Black Shales*. Mitteilungen aus dem Geologisch-Paläontologischen Institut, Universität Hamburg, Hamburg, Germany, pp. 205–246.
- Kuyper, M.M., Pancost, R.D., Damsté, J.S.S., 1999. A large and abrupt fall in atmospheric CO₂ concentration during Cretaceous times. *Nature* 399 (6734), 342–345. <https://doi.org/10.1038/20659>.
- Lamolda, M.A., Mao, S., 1999. The Cenomanian–Turonian boundary event and dinocyst record at Ganuza (northern Spain). *Paleogeogr. Palaeoclimatol. Palaeoecol.* 150 (1–2), 65–82. [https://doi.org/10.1016/S0031-0182\(99\)00008-5](https://doi.org/10.1016/S0031-0182(99)00008-5).
- Laugie, M., Donnadiu, Y., Ladant, J.B., Bopp, L., Ethé, C., Raison, F., 2021. Exploring the impact of Cenomanian paleogeography and marine gateways on oceanic oxygen. *Paleoceanogr. Paleoclimatol.* 36 (7), e2020PA004202 <https://doi.org/10.1029/2020PA004202>.
- Laurin, J., Barclay, R.S., Sageman, B.B., Dawson, R.R., Pagani, M., Schmitz, M., Eaton, J., McInerney, F.A., McElwain, J.C., 2019. Terrestrial and marginal-marine record of the mid-Cretaceous Oceanic Anoxic Event 2 (OAE 2): high-resolution framework, carbon isotopes, CO₂ and sea-level change. *Paleogeogr. Palaeoclimatol. Palaeoecol.* 524, 118–136. <https://doi.org/10.1016/j.palaeo.2019.03.019>.
- Leereveldt, H., 1995. Dinoflagellate cysts from the Lower Cretaceous Rio Argos succession (Doctoral dissertation thesis). Retrieved from Utrecht University Student Theses Repository. <https://studenttheses.uu.nl/browse>. Location: Universiteit Utrecht.
- Letolle, R.R., 1979. Oxygen 18 and Carbon 13 isotopes from the bulk carbonate samples, Leg 47B. *Initial Rep. Deep Sea Drill. Proj.* 47 (2), 493–496. <https://doi.org/10.2973/dsdp.proc.47-2.115.1979>.
- Li, Y.X., Montañez, I.P., Liu, Z., Ma, L., 2017. Astronomical constraints on global carbon-cycle perturbation during Oceanic Anoxic Event 2 (OAE2). *Earth Planet. Sci. Lett.* 462, 35–46. <https://doi.org/10.1016/j.epsl.2017.01.007>.
- Li, Y.X., Liu, X., Selby, D., Liu, Z., Montañez, I.P., Li, X., 2022. Enhanced ocean connectivity and volcanism instigated global onset of Cretaceous Oceanic Anoxic

- Event 2 (OAE2)~ 94.5 million years ago. *Earth Planet. Sci. Lett.* 578, 117331. <https://doi.org/10.1016/j.epsl.2021.117331>.
- Louail, M.J., Bellier, J.-P., Damotte, R., Durand, S., 1978. Stratigraphie du Cénomane littoral de la Marge Sud-Ouest du Bassin de Paris. L'exemple du sondage de Loudun. *Géologie Méditerranéenne* 5, 115–124.
- Lowery, C.M., Self-Trail, J.M., Barrie, C.D., 2021. Enhanced terrestrial runoff during Oceanic Anoxic Event 2 on the North Carolina Coastal Plain, USA. *Clim. Past* 17 (3), 1227–1242. <https://doi.org/10.5194/cp-17-1227-2021>.
- Lubimova, K.A., Samoilovich, S.R., 1975. Palaeocene epoch. In: Zauer, V.V. (Ed.), *Palaeophytogeography of the North of the U.S.S.R. during the Cretaceous and Palaeogene*. Tr. VNIGRI [In Russian], Moscow, Russia, pp. 49–54.
- Masure, E., 1984. L'indice de diversité et les dominances des "communautes" de kystes de Dinoflagellés; marqueurs bathymétriques; forage 398 D, croisière 47 B. *Bulletin de la Société géologique de France* 7 (1), 93–111. <https://doi.org/10.2113/gssgfbull.S7-XXVI.1.93>.
- Méon, H., Guignard, G., Pacltová, B., Svobodová, M., 2004. Normapolles. Comparison between central and southwestern Europe during the Cenomanian and Turonian: evolution of biodiversity and paleoenvironment. *Bulletin de la Société Géologique de France* 175 (6), 579–593. <https://doi.org/10.2113/175.6.579>.
- Meyers, S.R., Sageman, B.B., Arthur, M.A., 2012. Obliquity forcing of organic matter accumulation during Oceanic Anoxic Event 2. *Paleoceanography* 27 (3). <https://doi.org/10.1029/2012PA002286>.
- Monnet, C., 2009. The Cenomanian–Turonian boundary mass extinction (late Cretaceous): new insights from ammonoid biodiversity patterns of Europe, Tunisia and the Western Interior (North America). *Palaeogeogr. Palaeoclimatol. Palaeoecol.* 282, 88–104. <https://doi.org/10.1016/j.palaeo.2009.08.014>.
- Monteiro, F.M., Pancost, R.D., Ridgwell, A., Donnadieu, Y., 2012. Nutrients as the dominant control on the spread of anoxia and euxinia across the Cenomanian–Turonian oceanic anoxic event (OAE2): model-data comparison. *Paleoceanography* 27 (4). <https://doi.org/10.1029/2012PA002351>.
- Moullade, M., Applegate, J.L., Bergen, J.A., Thurow, J., Doyle, P.S., Drugg, W.S., Habib, D., Masure, E., Ogg, J., Taugourdeau-Lantz, J., 1988. Ocean drilling program Leg 103 biostratigraphic synthesis. *Proceedings of the Ocean Drilling Program, Scientific Results* 103, 685–695. <https://doi.org/10.2973/odp.proc.sr.103.176.1988>.
- Mudie, P.J., McCarthy, F.M., 2006. Marine palynology: potentials for onshore–offshore correlation of Pleistocene–Holocene records. *Trans. R. Soc. S. Afr.* 61 (2), 139–157. <https://doi.org/10.1080/00359190609519964>.
- Murillas, J., Mougnot, D., Boulot, G., Comas, M.C., Banda, E., Mauffret, A., 1990. Structure and evolution of the Galicia Interior Basin (Atlantic western Iberian continental margin). *Tectonophysics* 184 (3–4), 297–319. [https://doi.org/10.1016/0040-1951\(90\)90445-E](https://doi.org/10.1016/0040-1951(90)90445-E).
- Pacltová, B., 1971. Palynological study of Angiospermae from the Peruc Formation (? Albian–Lower Cenomanian) of Bohemia. *Sborník Geologických Ved Rada P Paleontologie* 13, 105–138.
- Pacltová, B., 1978. Paleobiology and natural selection. In: *Proceedings, Symposium Natural Selection*, Liblice, CSAV, Praha, pp. 207–217.
- Pavlishina, P., Wagreich, M., 2012. Biostratigraphy and paleoenvironments in a northwestern Tethyan Cenomanian–Turonian boundary section (Austria) based on palynology and calcareous nannofossils. *Cretac. Res.* 38, 103–112. <https://doi.org/10.1016/j.cretres.2012.02.005>.
- Pearce, M.A., Jarvis, I., Tocher, B.A., 2009. The Cenomanian–Turonian boundary event, OAE2 and palaeoenvironmental change in epicontinental seas: new insights from the dinocyst and geochemical records. *Palaeogeogr. Palaeoclimatol. Palaeoecol.* 280 (1–2), 207–234. <https://doi.org/10.1016/j.palaeo.2009.06.012>.
- Peyrot, D., Barrón, E., Comas-Rengifo, M.J., Barroso-Barcenilla, F., Feist-Burkhardt, S., 2008. Palinología del tránsito Cenomaniense/Turonense en la sección de Puente de (Burgos, España). *Coloquios de Paleontología* 58, 101–161.
- Peyrot, D., Barroso-Barcenilla, F., Barrón, E., Comas-Rengifo, M.J., 2011. Palaeoenvironmental analysis of Cenomanian–Turonian dinocyst assemblages from the Castilian Platform (northern-central Spain). *Cretac. Res.* 32 (4), 504–526. <https://doi.org/10.1016/j.cretres.2011.03.006>.
- Peyrot, D., Barroso-Barcenilla, F., Feist-Burkhardt, S., 2012. Palaeoenvironmental controls on late Cenomanian–early Turonian dinoflagellate cyst assemblages from Condemios (Central Spain). *Rev. Palaeobot. Palynol.* 180, 25–40. <https://doi.org/10.1016/j.revpalbo.2012.04.008>.
- Peyrot, D., Barrón, E., Polette, F., Batten, D.J., Néraudeau, D., 2019. Early Cenomanian palynofloras and inferred resiniferous forests and vegetation types in Charentes (southwestern France). *Cretac. Res.* 94, 168–189. <https://doi.org/10.1016/j.cretres.2018.10.011>.
- Philippe, M., Gomez, B., Girard, V., Coiffard, C., Daviero-Gomez, V., Thevenard, F., Billon-Bruyat, J.P., Guimard, M., Latil, J.L., Le Loeuff, J., Néraudeau, D., Olivero, D., Schlögl, J., 2008. Woody or not woody? Evidence for early angiosperm habit from the Early Cretaceous fossil wood record of Europe. *Palaeoworld* 17 (2), 142–152. <https://doi.org/10.1016/j.palwor.2008.06.001>.
- Powell, A.J. (Ed.), 1992. *A Stratigraphic Index of Dinoflagellate Cysts*. Chapman & Hall, London, pp. 155–251.
- Ravn, R.L., 1995. Miospores from the muddy sandstone (upper Albian), wind river basin, Wyoming, U.S.A. *Palaeontogr. Abt. B* 234 (3–6), 41–91.
- Retallack, G.J., 2001. A 300-million-year record of atmospheric carbon dioxide from fossil plant cuticles. *Nature* 411 (6835), 287–290. <https://doi.org/10.1038/35077041>.
- Robbins, E.L., Perry Jr., W.J., Doyle, J.A., 1975. Palynological and stratigraphic investigations of four deep wells in the Salisbury Embayment of the Atlantic Coastal Plain. In: *US Geological Survey*, 75–307. <https://doi.org/10.3133/ofr75307>.
- Robinson, S.A., Heimhofer, U., Hesselbo, S.P., Petrizzo, M.R., 2017. Mesozoic climates and oceans—a tribute to Hugh Jenkyns and Helmut Weissert. *Sedimentology* 64 (1), 1–15. <https://doi.org/10.1111/sed.12349>.
- Robinson, S.A., Dickson, A.J., Pain, A., Jenkyns, H.C., O'Brien, C.L., Farnsworth, A., Lunt, D.J., 2019. Southern Hemisphere Sea-surface temperatures during the Cenomanian–Turonian: Implications for the termination of Oceanic Anoxic Event 2. *Geology* 47 (2), 131–134. <https://doi.org/10.1130/G45842.1>.
- Rodríguez-Barreiro, I., Santos, A.A., Arribas, M.E., Mas, R., Arribas, J., Villanueva-Amadoz, U., Fernández-Balador, F.T., Díez, J.B., 2022. The Jurassic–Cretaceous transition in the West Cameros Basin (Tera Group, Burgos, Spain): sedimentological and palynostratigraphical insights. *Cretac. Res.* 139, 105300. <https://doi.org/10.1016/j.cretres.2022.105300>.
- Ryan, W.B.F., Sibuet, J.-C., Arthur, M.A., Lopatin, B.G., Moore, D.G., Maldonado, A., et al., 1979a. Introduction and explanatory notes. Initial Rep. Deep Sea Drill. Proj. 47 (2), 25–233. <https://doi.org/10.2973/dsdp.proc.47-2.101.1979>.
- Ryan, W.B.F., Sibuet, J.-C., Arthur, M.A., Lopatin, B.G., Moore, D.G., Maldonado, A., et al., 1979b. Site 398. Initial Rep. Deep Sea Drill. Proj. 47 (2), 25–233. <https://doi.org/10.2973/dsdp.proc.47-2.102.1979>.
- Sames, B., Wagreich, M., Wendler, J.E., Haq, B.U., Conrad, C.P., Melinte-Dobrinescu, M. C., Hu, X., Wendler, I., Wolfring, E., Yilmaz, I.O., Zorina, S.O., 2016. Short-term sea-level changes in a greenhouse world—a view from the Cretaceous. *Palaeogeogr. Palaeoclimatol. Palaeoecol.* 441, 393–411. <https://doi.org/10.1016/j.palaeo.2015.10.045>.
- Sánchez-Pellicer, R., Masure, E., Villier, L., 2018. Distribution of Albian dinoflagellate cyst associations along a proximal–distal transect across the Iberian margin. *Cretac. Res.* 92, 240–256. <https://doi.org/10.1016/j.cretres.2018.08.004>.
- Santos, A.A., Villanueva-Amadoz, U., Royo-Torres, R., Sender, L.M., Cobos, A., Alcalá, L., Díez, J.B., 2018. Palaeobotanical records associated with the first dinosaur defined in Spain: palynostratigraphy, taxonomy and palaeoenvironmental remarks. *Cretac. Res.* 90, 318–334. <https://doi.org/10.1016/j.cretres.2018.04.023>.
- Santos, A.A., Nel, A., Rodríguez-Barreiro, I., Sender, L.M., Wappler, T., Díez, J.B., 2022a. Insect and plant diversity in hot-spring ecosystems during the Jurassic–Cretaceous boundary from Spain (Aguilar Fm., Palencia). *Biology* 11 (2), 273. <https://doi.org/10.3390/biology11020273>.
- Santos, A.A., Piñuela, L., Rodríguez-Barreiro, I., García-Ramos, J.C., Díez, J.B., 2022b. Palynology from “The Jurassic Dinosaur Coast” of Asturias (Lastres Fm., Northwestern Spain): palynostratigraphical and palaeoecological insights. *Biology* 11 (12), 1695. <https://doi.org/10.3390/biology11121695>.
- Schlanger, S.O., Jenkyns, H.C., 1976. Cretaceous oceanic anoxic events: causes and consequences. *Geol. Mijnb.* 55 (3–4), 179–184.
- Scholle, P.A., Arthur, M.A., 1980. Carbon isotope fluctuations in Cretaceous pelagic limestones: potential stratigraphic and petroleum exploration tool. *AAPG Bull.* 64 (1), 67–87. <https://doi.org/10.1306/2F91892D-16CE-11D7-8645000102C1865D>.
- Sigal, J., 1979. Chronostratigraphy and eocstratigraphy of Cretaceous formations recovered on DSDP Leg 47B, Site 398. Initial Rep. Deep Sea Drill. Proj. 47 (2), 287–326. <https://doi.org/10.2973/DSDP.PROC.47-2.105.1979>.
- Sinton, C.W., Duncan, R.A., 1997. Potential links between ocean plateau volcanism and global ocean anoxia at the Cenomanian–Turonian boundary. *Econ. Geol.* 92 (7–8), 836–842. <https://doi.org/10.2113/gsecongeo.92.7-8.836>.
- Smith, A.R., Pryer, K.M., Schuettpelz, E., Korall, P., Schneider, H., Wolf, P.G., 2006. A classification for extant ferns. *Taxon* 55, 705–731. <https://doi.org/10.2307/25065646>.
- Snow, L.J., Duncan, R.A., Bralower, T.J., 2005. Trace element abundances in the Rock Canyon Anticline, Pueblo, Colorado, marine sedimentary section and their relationship to Caribbean plateau construction and oxygen anoxic event 2. *Paleoceanography* 20, 3. <https://doi.org/10.1029/2004PA001093>.
- Svobodová, M., Méon, H., Pacltová, B., 1998. Characteristics of palynofloras of the Upper Cenomanian–Lower Turonian (anoxic facies) of the Bohemian and Vocontian Basins. *Bull. Czech Geol. Surv.* 73 (3), 229–251.
- Taugourdeau-Lantz, J., Azéma, C., Hasenboehler, B., Masure, E., Moron, J.M., 1982. Evolution des domaines continentaux et marins de la marge portugaise (Leg 47B, site 398D) au cours du Crétacé; Essai d'interprétation par l'analyse palynologique comparee. *Bulletin de la Société Géologique de France* 7 (3), 447–459. <https://doi.org/10.2113/gssgfbull.S7-XXIV.3.447>.
- Thurow, J., 1988. Cretaceous radiolarians of the North Atlantic Ocean: ODP Leg 103 (sites 638, 640, and 641) and DSDP Legs 93 (site 603) and 47B (site 398). *Proc. Ocean Drilling Prog. Scient. Results* 103, 379–418. <https://doi.org/10.2973/odp.proc.sr.103.148.1988>.
- Thurow, J., Moullade, M., Brumsack, H.J., Masure, E., Taugourdeau-Lantz, J., Dunham, K., 1988. The Cenomanian/Turonian boundary event (CTBE) at Hole 641A, ODP Leg 103 (compared with the CTBE interval at Site 398). *Proc. Ocean Drilling Prog. Scient. Results* 103, 587–634. <https://doi.org/10.2973/odp.proc.sr.103.172.1988>.
- Traverse, A., 1994. *Sedimentation of Land-Derived Palynomorphs in the Trinity-Galveston Bay Area, Texas. Sedimentation of Organic Particles*. Cambridge University Press, Cambridge, pp. 69–102. <https://doi.org/10.1017/CBO9780511524875.007>.
- Turgeon, S.C., Creaser, R.A., 2008. Cretaceous Oceanic Anoxic Event 2 triggered by a massive magmatic episode. *Nature* 454 (7202), 323–326. <https://doi.org/10.1038/nature07076>.
- Uličný, D., Kvaček, J., Svobodová, M., Špičáková, L., 1997. High-frequency sea-level fluctuations and plant habitats in Cenomanian fluvial to estuarine succession: Pecinov quarry, Bohemia. *Palaeogeogr. Palaeoclimatol. Palaeoecol.* 136 (1–4), 165–197. [https://doi.org/10.1016/S0031-0182\(97\)00033-3](https://doi.org/10.1016/S0031-0182(97)00033-3).
- Vakhrameev, V.A., 1970. Range and palaeoecology of Mesozoic conifers, the Cheirolepidiaceae. *Paleontol. Zh.* 1, 19–34.

- van Amerom, H.W.J., 1965. Upper-cretaceous pollen and spores assemblages from the so-called "Wealden" of the Province of Leon (Northern Spain). *Pollen Spores* 7 (1), 93–133.
- van Helmond, N.A., Ruvalcaba Baroni, I., Sluijs, A., Sinninghe Damsté, J.S., Slomp, C.P., 2014a. Spatial extent and degree of oxygen depletion in the deep proto-North Atlantic basin during Oceanic Anoxic Event 2. *Geochim. Geophys. Geosyst.* 15 (11), 4254–4266. <https://doi.org/10.1002/2014GC005528>.
- van Helmond, N.A., Sluijs, A., Reichert, G.J., Sinninghe Damsté, J.S., Slomp, C.P., Brinkhuis, H., 2014b. A perturbed hydrological cycle during Oceanic Anoxic Event 2. *Geology* 42 (2), 123–126. <https://doi.org/10.1130/G34929.1>.
- van Helmond, N.A., Sluijs, A., Papadomanolaki, N.M., Plint, A.G., Gröcke, D.R., Pearce, M.A., Eldrett, J.S., Trabucho-Alexandre, J., Walaszczyk, I., van de Schootbrugge, B., Brinkhuis, H., 2016. Equatorward phytoplankton migration during a cold spell within the Late Cretaceous super-greenhouse. *Biogeosciences* 13 (9), 2859–2872.
- Versteegh, G.J.M., 1994. Recognition of cyclic and non-cyclic environmental changes in the Mediterranean Pliocene: a palynological approach. *Mar. Micropaleontol.* 23 (2), 147–183. [https://doi.org/10.1016/0377-8398\(94\)90005-1](https://doi.org/10.1016/0377-8398(94)90005-1).
- Villanueva-Amadoz, U., . Nuevas aportaciones palinoestratigráficas para el intervalo Albense-Cenomaniense en el Sector NE de la Península Ibérica. Implicaciones paleogeográficas y paleoclimáticas (Doctoral dissertation). Retrieved from Dialnet. <https://dialnet.unirioja.es/servlet/tesis?codigo=205684>. Universidad de Zaragoza.
- Ward, J.V., 1986. Early Cretaceous angiosperm pollen from the Cheyenne and Kiowa formations (Albian) of Kansas, USA. *Palaeontogr. Abt. B* 202 (1–6), 1–81.
- Watson, J., Alvin, K.L., 1996. An English Wealden floral list, with comments on possible environmental indicators. *Cretac. Res.* 17 (1), 5–26.
- Williams, G.L., 1993. Morphology and stratigraphic ranges of selected Mesozoic–Cenozoic dinoflagellate taxa in the Northern Hemisphere. *Geol. Surv. Can. Pap.* 92 (10), 137.
- Williams, G.L., Brinkhuis, H.M.A.P., Pearce, M.A., Fensome, R.A., Weegink, J.W., Exon, N.F., 2004. Southern Ocean and global dinoflagellate cyst events compared: index events for the Late Cretaceous–Neogene. *Proc. Ocean Drilling Prog. Scient. Results* 189, 1–98. <https://doi.org/10.2973/odp.proc.sr.189.107.2004>.
- Wingate, F.H., 1980. Plant microfossils from the Denton Shale Member of the Bokchito Formation (Lower Cretaceous, Albian) in southern Oklahoma. *Oklahoma Geol. Surv. Bull.* 130, 1–93.
- Winterer, E.L., Gee, J.S., Van Waasbergen, R.J., Boillot, G., 1988. The source area for Lower Cretaceous clastic sediments of the Galicia margin: geology and tectonic and erosional history. *Proc. Ocean Drilling Prog. Scient. Results* 103, 697–732. <https://doi.org/10.2973/odp.proc.sr.103.181.1988>.
- Witkowski, C.R., Weijers, J.W.H., Blais, B., Schouten, S., Sinninghe Damsté, J.S., 2018. Molecular fossils from phytoplankton reveal secular pCO₂ trend over the Phanerozoic. *Sci. Adv.* 4 (11), eaat4556 <https://doi.org/10.1126/sciadv.aat4556>.
- Wolfe, J.A., Pakiser, H.M., 1971. Stratigraphic interpretations of some Cretaceous microfossil floras of the Middle Atlantic States. *US Geological Survey Professional Paper* 750, B35–B47.
- Wood, G.D., Gabriel, A.M., Lawson, J.C., 1996. Palynological techniques-processing and microscopy. In: Jansonius, J., McGregor, D.C. (Eds.), *Palynology: Principles and Applications*, vol. 1. American Association of Stratigraphic Palynologists Foundation, Dallas, TX, pp. 29–50.
- Zaklinskaya, E.D., 1977. Pokrytosemennyye po palinologicheskim dannym [Angiosperms based on palynological data]. In: Vakrameev, V.A. (Ed.), *Razvitie flor na granitse Mesozoya Kainozoya [Floral Evolution at the Mesozoic–Cenozoic Boundary]*. Nauka, Moscow, pp. 66–119 (in Russian).
- Zhang, J., Lenz, O.K., Wang, P., Hornung, J., 2021. The Eco-Plant model and its implication on Mesozoic dispersed sporomorphs for Bryophytes, Pteridophytes, and Gymnosperms. *Rev. Palaeobot. Palynol.* 293, 104503 <https://doi.org/10.1016/j.revpalbo.2021.104503>.